LASER INTERFEROMETER GRAVITATIONAL WAVE OBSERVATORY
- LIGO -
CALIFORNIA INSTITUTE OF TECHNOLOGY
MASSACHUSETTS INSTITUTE OF TECHNOLOGY

LIGO-E950099	**-04-D**	8/7/96
Doc Number	*Group-*	*Date*

Core Optics Components Requirements (1064 nm)

Bill Kells

DRAFT

This is an internal working note
of the LIGO Project
Distribution:
COC-DRR review board

California Institute of Technology
LIGO Project - MS 102-33
Pasadena CA 91125
Phone (818) 395-2966
Fax (818) 304-9834
E-mail: info@ligo.caltech.edu
WWW: http://www.ligo.caltech.edu

Signature Page

_____
........, COC Task Leader^{TBD}

ETC. TBD

1   INTRODUCTION

1.1. Purpose

This Design Requirements Document (DRD) for the Core Optics Components (COC) subsystem identifies the information necessary to define the COC subsystem and quantify its relationship to other LIGO subsystems. Requirements, formally flowing down from the Systems (SYS) task, are stated to provide a full description of the COC and their optical and physical properties. Each requirement specification will be justified in terms of its impact on the LIGO performance.

1.2. Scope

This document will detail only requirements on the 6 or 7 monolithic optical elements necessary for each LIGO interferometer. Reference to other related and interfacing subsystems will be made only to define interfaces, clarify the rationale for requirements, and allow a full justification of particular required parameters.

   The actual fabrication specifications for realizing the herein required optics and a program for developing and verifying their delivered performance (including the "Pathfinder" prototypes) will be presented in a companion COC Conceptual Design Document (LIGO-E950100-00-D).

   Part of the LIGO concept is to construct 2000 m, half arm length, IFOs as well as those of the full 4000 m length design. Explicit discussion of the requirements for the 2000 m IFO will be limited to section 3.2.1.8. Elsewhere it is tacit that reference is to the 4000 m version unless stated otherwise.

1.3. Definitions

1.3.1.   Physical Definitions

Physically, the COC subsystem consists of the following items as shown in Fig. 1:

1.3.1.1   Fused Silica cylindrical substrates:

- Test masses (TM) of two types: input TM (ITM) and end TM (ETM).
- Beam splitter (BS).
- Recycling mirror (RM).
- Folding mirrors (FM) which will be incorporated only into the 2000 m arm length IFO. See section 3.2.1.8.

1.3.1.2   Thin film optical coatings (applied to faces of the substrates 1.3.1.1):

- Anti reflection coating (ARxx) applied to surface 2 of each optic: e.g. ARBS= anti-reflection coating on surface BS2 of the BS substrate.

- Enhanced reflectance coating (ERxx) applied to surface 1 of each optic: e.g. ERITM = reflec-

tor coating on input test mass.

- Any coating applied to any portion of the substrate surface (e.g. substrate sides) for mitigating localized surface charging**TBD**(dielectric surface charging is recognized as a potentially serious problem. See 1.5.1.8).
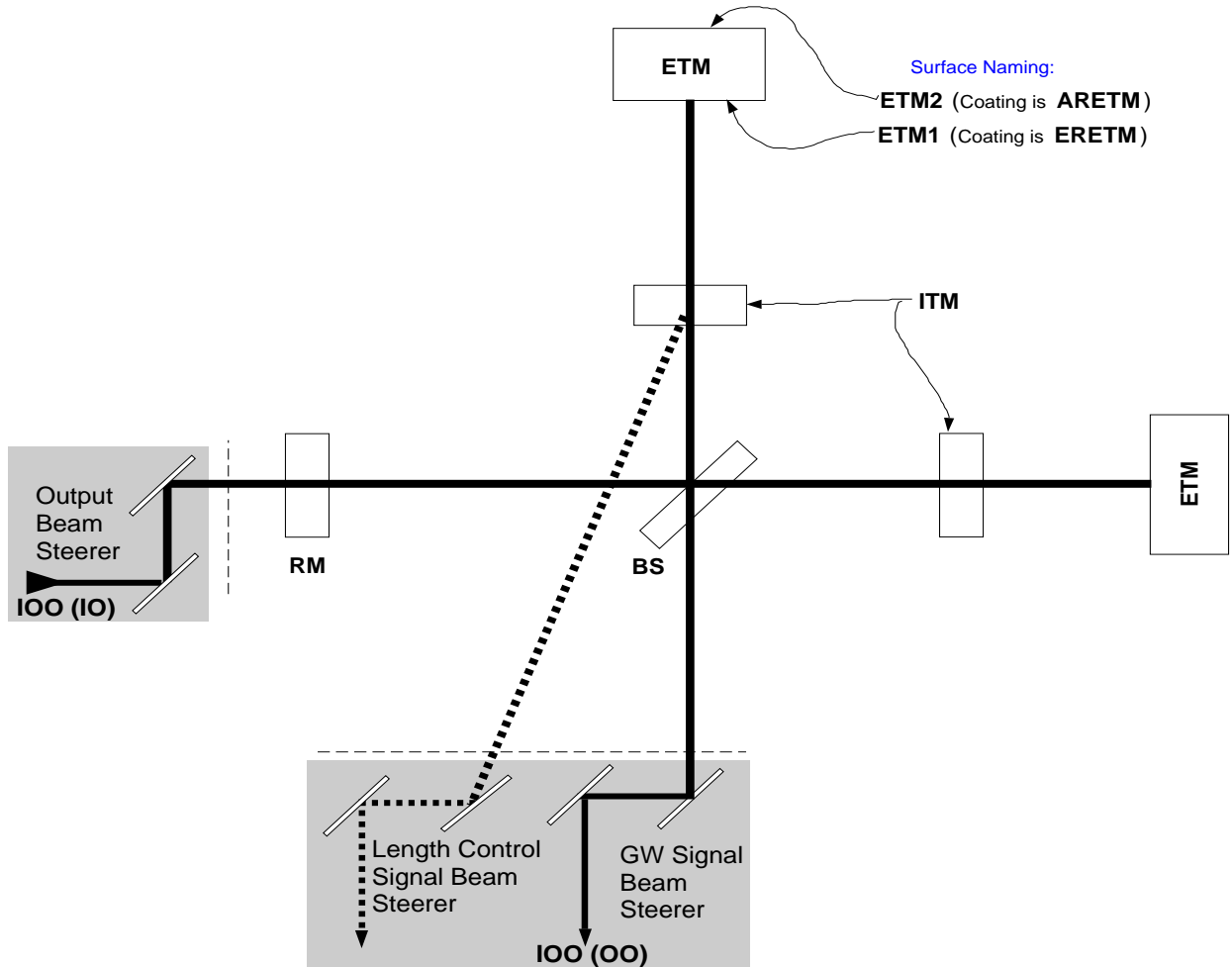

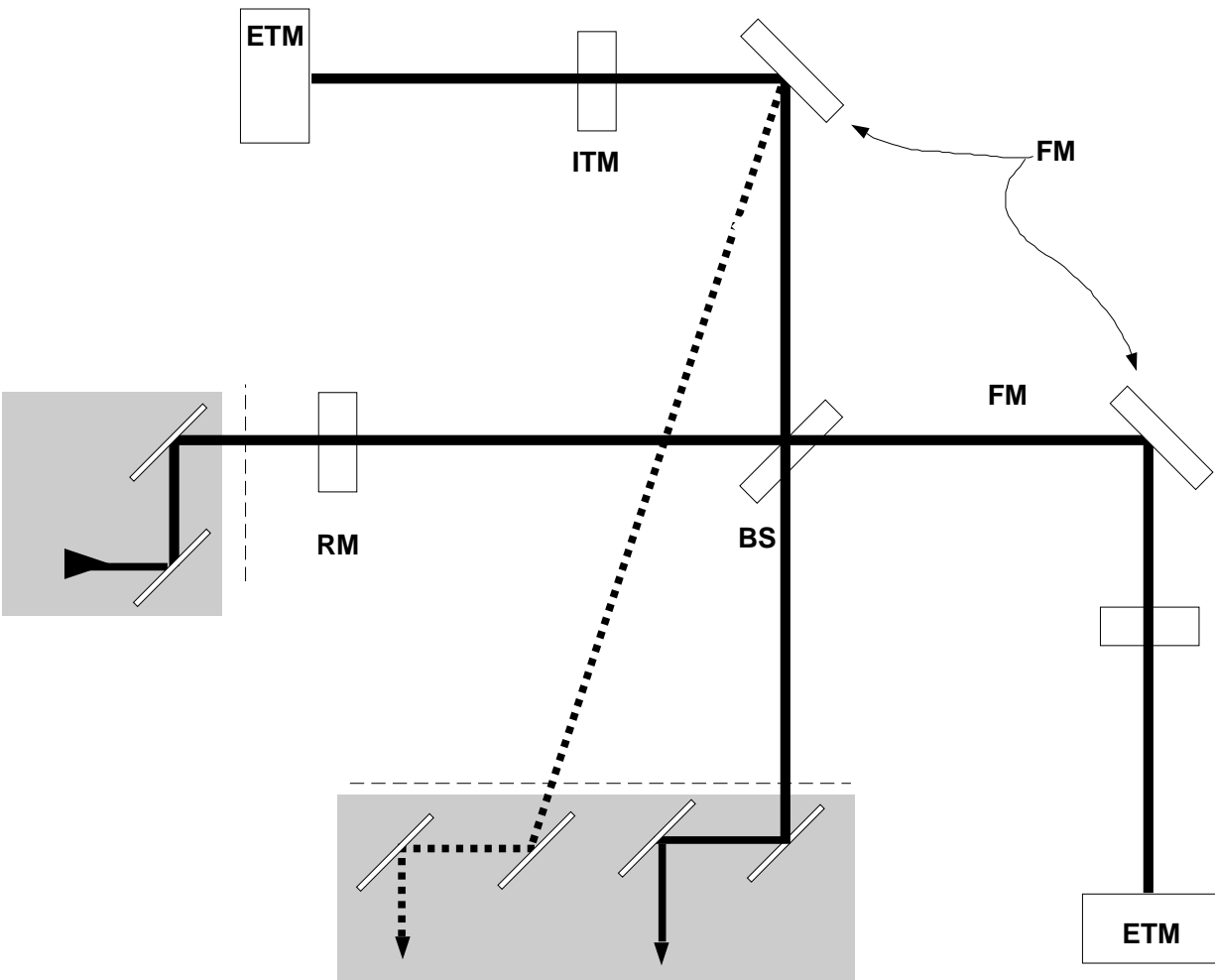**Figure 1: Physical definition of COC (4000 m IFO)**

Figure 2: Physical definition of COC (2000 m IFO)

1.4. Acronyms

- Throughout this document items will be mentioned whose existence, scope, or value are yet to be determined. A symbol ^{TBD} represents this status.
- IFO= Interferometer
- SUS= Suspension design system.
- IOO= Input optics. This subsystem contains subdivisions (OO) for output optics and (IO) for input optics.
- ASC= Alignment sensing and control subsystem.
- YAG= 1.06 micron laser or laser light (wavelength λ if not otherwise specified).

- SYS= Detector Systems Engineering/Integration.
- λ_s = optical surface spatial wavelength.
- GW= gravitational wave.
- G= Power recycling cavity gain: G_c for carrier power; G_{sb} for side band power
- CD= Contrast defect: CD_c for carrier power; CD_{sb} for side band power.
- w_0 = Primary cavity's beam Gaussian waist radius. w_{xx} indicates beam Gaussian radius at location xx. For example w_{ETM} will be the end test mass beam radius.
- R_{eff}= the effective radius of curvature for a mirror surface as seen by an incident Gaussian beam. (see 3.2.1.4.1 for further definition)
- ϕ, d, = diameter, thickness of optics. ϕ_s, d_s would specify substrate diameter and thickness
- HTM= higher transverse modes.
- OSEM: Servo actuators (5 per COC) which keep elements in alignment.
- FFT model: the standard MIT computer simulation of the static LIGO IFO
- "in-line" and "out-line": refer to the two LIGO IFO arm. The in-line arm is the one colinear with the RM-BS axis.

1.5. Applicable Documents

1.5.1. LIGO Documents

1.5.1.1   COC centering Requirement: LIGO-T950049-00-D

1.5.1.2   LIGO Science Requirements Document: LIGO-E950018-00-E

1.5.1.3   SUS Design Requirements Document: LIGO-T950011-06-D

1.5.1.4   COC Conceptual Design Document: LIGO-T950100-00-D

1.5.1.5   ASC Design Requirements Document: LIGO-T952007-00-D.

1.5.1.6   COC sizes meetings notes: LIGO-L960112

1.5.1.7   Optical Wave front Distortion Specification notes (R. Weiss) LIGO-T952009-00-E

1.5.1.8   Electrostatic Charging on TMs (FJR) L960044-00-E

1.5.1.9   AR/ER coating properties (H. Yamamoto) LIGO-G950043

1.5.1.10   FFT model description (B. Bochner, Y. Hefetz) LIGO-G950061-01-R**.**

1.5.2. Non-LIGO Documents

1.5.2.1   VIRGO Final Design (report) ver 0. June 1995

1.5.2.2   Thesis, P. Hello. University of Paris, 1994.

1.5.2.3   W. Winkler,et. al., Optics Comm.,**112**, 245(1994).

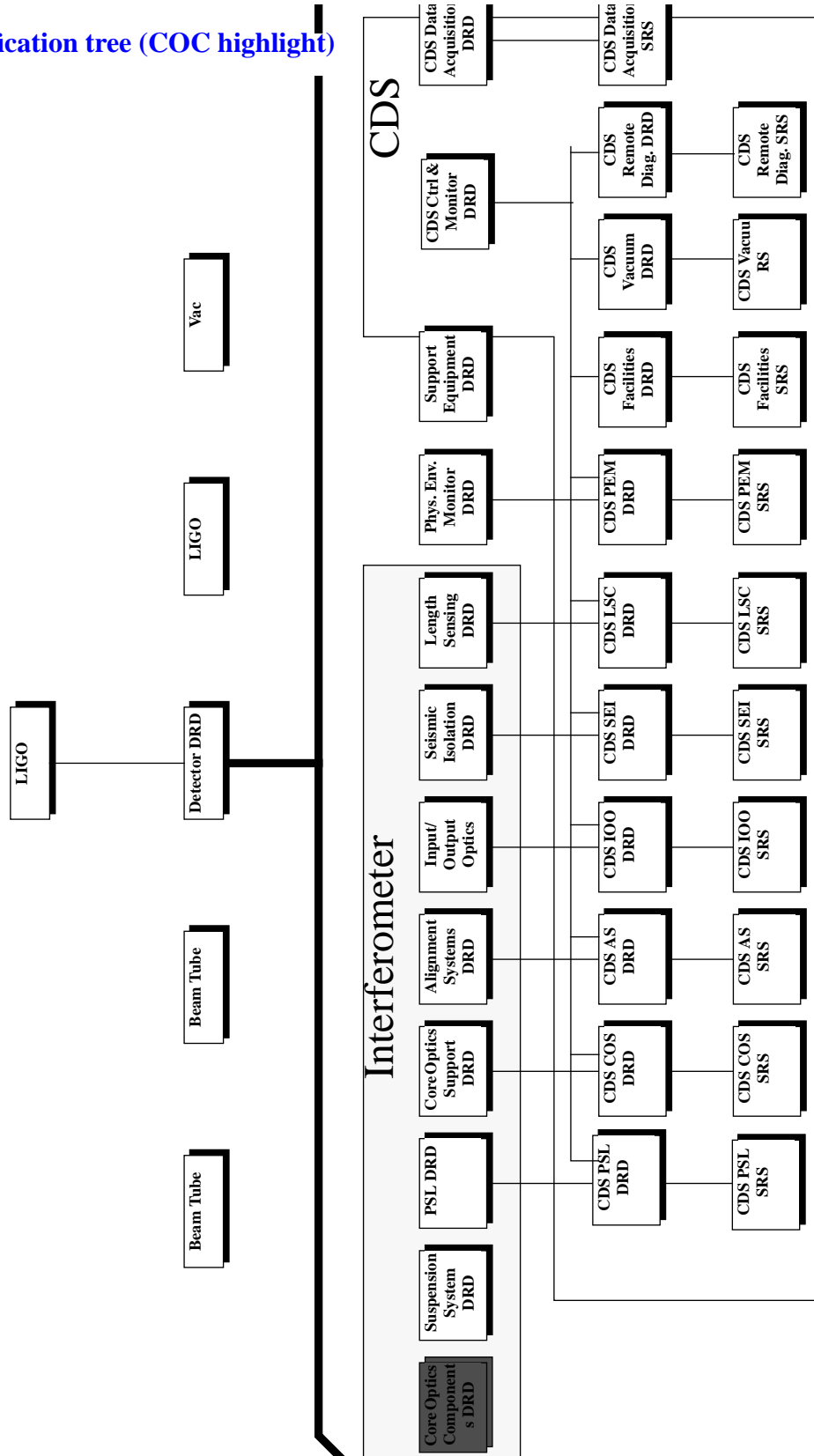1.5.2.4   W. Winkler, et. al., Phys. Rev. **A44**, 7022

2   GENERAL DESCRIPTION

2.1. Specification Tree

This document is part of an overall LIGO detector requirement specification tree (originating from SYS). This particular document is highlighted in figure 3.

2.2. Product Perspective

3: Specification tree (COC highlight)

The COC manipulates the IOO laser light beam into a form suitable for the optimal detection of gravitational waves within the LIGO design bandwidth. Thus the COC interfaces optically with the IOO subsystem. COC are aligned via optical (laser) interface with sensing systems provided by ASC (see figure 8). The only mechanical interface is to COS (specified by the SUS DRD) via contacting suspension elements and position/orientation control components (figure7, and 1.5.1.3). There is no direct connection to CDS (no electrical signals into or out off COC).
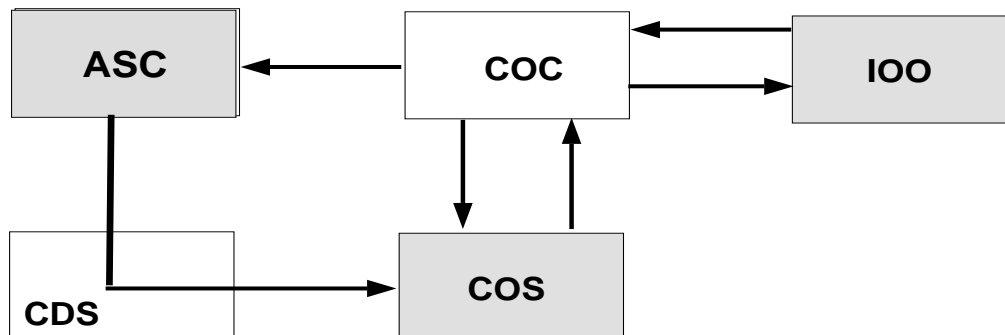

Figure 4: Subsystem relationship to COC

 The COC performance depends essentially on the quality of its primary optical surfaces. Preserving the fabricated quality of these surfaces will be crucial. A dominant LIGO design feature must be to control the potential for contamination of the COC optical surfaces.

2.3. Product Functions

The main functions of the COC are:

- Provide a high performance TEM_{00} mode optical cavity interferometer (IFO), which is maximally sensitive to gravitational waves.
- Provide appropriate optical ports which allow routing of samples of the optical cavity light of optimal intensity and phase to various gravitational wave, length and alignment sensing detectors.
- Minimize stray/scattered light from the optical cavities and surfaces.
- Minimize the effect of thermal mode noise from both the optic's internal modes and the interfacing suspension (SUS) components.
- Allow optimal match of the IOO beam TEM_{00} mode structure to the fundamental mode of the IFO cavities.

2.4. General Constraints

Realistic feasibility constraints have guided the nature of the requirements from the outset of the LIGO program. We mention the main ones here:

2.4.1.   Simplicity

The basic GW IFO configuration, specified by SYS, should be simple in terms of COC number and type multiplicity:

- each [imperfect] optic contributes additional wave front distortion, which degrades perfor-

mance.
- Each COC optic necessitates an additional [noisy] control servo and suspension system, which degrades performance.
- Contamination potential is proportionally reduced.
- Overall system design is significantly eased, clear optical lines of sight are increased, etc.
- Physically (size, material, finish, etc.) identical or similar COC are expected to greatly simplify optical fabrication, IFO construction, spares inventory, and handling fixturing and testing.

This document assumes a minimal IFO component count (figure 1) comprising two optics in each arm cavity (minimum possible); and two additional ones (four for the 2000m IFOs).

2.4.2. Basic Shape

The COC are to be fabricated within the constraints of the ultra high precision optical industry. This framework virtually determines the choice of substrate geometrical shape (circular cylinder, possibly with wedge faces). Additional reasons for this shape include:

- The natural shape for the COC optical faces is circular, matching the TEM_{00} mode symmetry.
- This also is the practical requirement for suspension by wire loop.
- Understanding of the internal mechanical mode spectrum and influence is simplified by this choice.

We therefore assume without further detailed discussion that the all COC are of the basic right circular cylinder shape.

2.4.3. Continuous operation

LIGO must operate with high availability, therefore the COC must be designed with high reliability and low mean time to repair. (Note that this is a general statement, and the MTBF and MTTR will be exactly specified in Section 3).

2.4.4. Substrate material

Fused silica (FS) is chosen as the COC substrate material due to the vast body of optical industry and LIGO experience with this material.

2.5. Assumptions and Dependencies

- The primary laser beam light is at 1064 nm (YAG).
- A curved-curved arm cavity configuration with cavity length = 4000 m, and $g_1 g_2 = 1/3$ is assumed. The case of a 2000 m length arm cavity IFO will be discussed separately in 3.2.1.7
- The two IFO arm cavities are oriented in the same plane at 90°. This requires a 45° oriented BS element. This BS is assumed to split the two arm beams in the coating on its front surface.
- That all COC are fabricated from high purity and homogeneity grade fused silica (see 3.2.1.5)
- That the primary optical ER and AR coatings on the COC substrates will be of the dielectric multilayer hard oxide thin film technology (see 3.2.1.3).
- All COC will be mounted by hanging in wire loop suspension assemblies (see figure 7).

- All COC are of the right circular cylinder form (with only slight departure as described in 3.2.1.1).
- All COC optical surfaces are to have nominally flat surfaces except for the primary (ER) ETM, ITM, and RM surfaces which are assumed to be sections of spheres with R_{eff} (see table 1) adjusted to maintain arm cavity $g_1 g_2 = 1/3$.
- The (IOO) beam entering the IFO will be polarized such that its electric field is normal to the plane of the IFO. Principally this affects the specification of the non-normal incidence COC, that is the beam splitter the fold mirrors and any pick-off mirrors.

3 REQUIREMENTS

3.1. Introduction

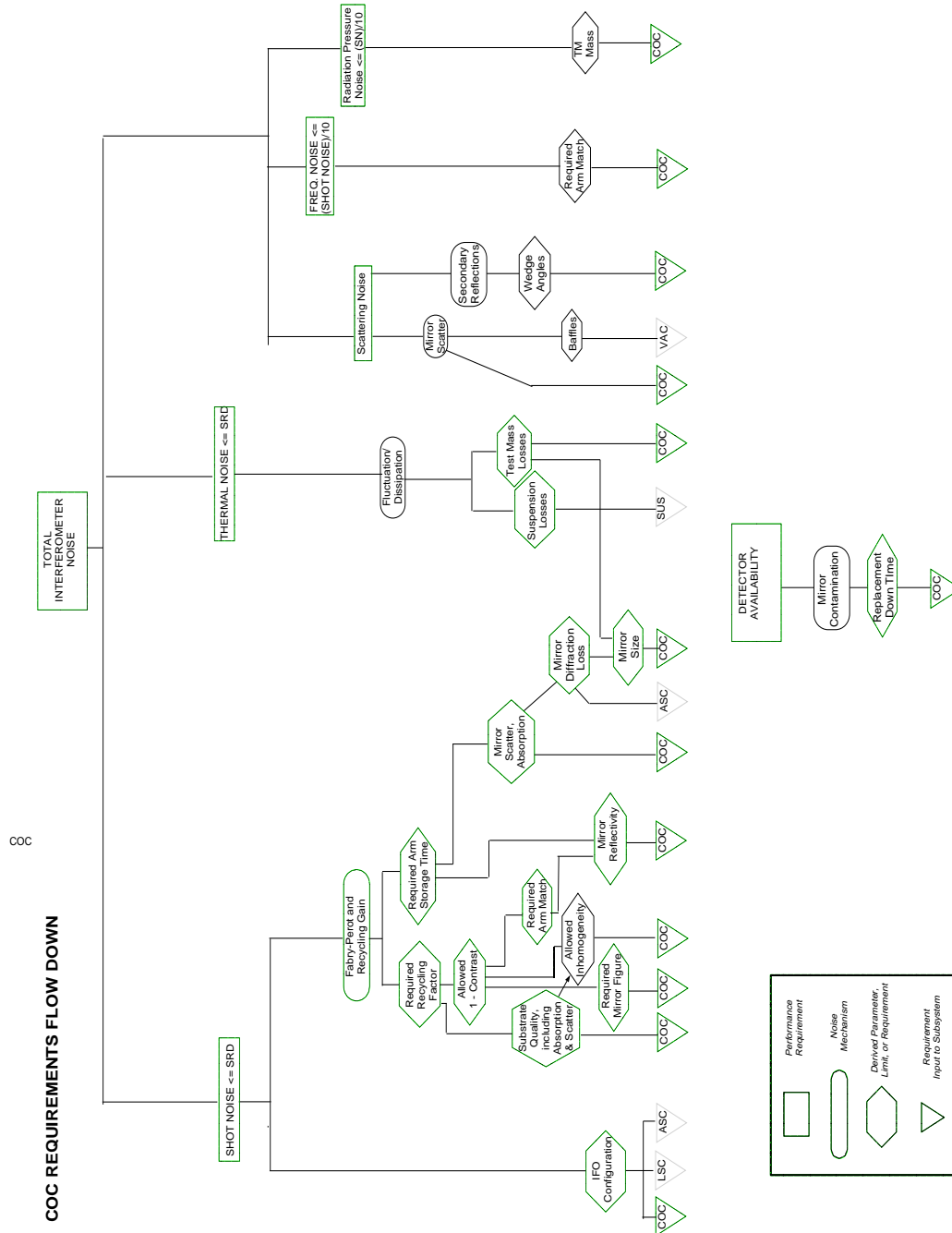Figure 4 is a requirements flow down tree from Detector Systems Integration to the COC .

Figure 5: Requirements flow down to COC

Primarily the COC requirements flow down from those determined by SYS to be appropriate for the LIGO IFO to reach its target goals as a GW detector. Of only secondary consideration (for example if there is minimal impact on attaining the primary specifications) are requirements for optimal engineering of other subsystem components. For instance the specification of wedge angles for the TM surface 2 to facilitate implementation of the LSC and ASC sensing systems is strictly subordinate to this specification not [negatively] impacting the TM optical cavity performance. Table 8 summarizes such flow down from primary (SYS) requirements of the detector (or subsystems) to requirements of COC and other subsystems.

Table 1: Performance requirement flow down

Requirement on COC	Other Subsystem	Other Subsystem Requirement Category	Primary Requirement Mechanism
Number of pick-off surfaces for length control	SYS	IFO configuration	Necessity of inter cavity signal for orientation & length control
Folding mirror number	SYS	IFO configuration	Number of interferometers per site.
Substrate bulk optical quality	SYS	IFO Cavity Power gains	Minimize loss to bulk scattering mechanisms
Element optical surface quality			Minimize loss to surface scatter out of TEM$_{00}$
Substrate bulk optical quality	SYS	Dark port contrast defect	Wave front distortion: bulk inhomogeneities
Element optical surface quality			Wave front distortion: surface irregularities
Coating absorption	SYS	Arm cavity intensity limitation.	Minimize thermal distortion of elements.
Element diameters	SYS	Recycling cavity power gain	Optimum substrate Via. Optimum effective optical Via.
		Restarting loss to baffles	
Substrate bulk mechanical & chemical quality	SYS	IFO thermal noise from substrate fluctuation-dissipation	Maximize substrate material Qs.
Substrate dimensions			Internal mode resonant frequencies
Secondary surface AR reflectivity & wedge angle	SYS	Stray light beam control and restarted light noise	Generation of ghost beams from secondary surfaces

Table 1: Performance requirement flow down

Requirement on COC	Other Subsystem	Other Subsystem Requirement Category	Primary Requirement Mechanism
AR reflectivity & wedge angles	ASC & LSC	Signals for length and orientation control servos	Select ghost beams of desired properties
ETM reflectivity			
Mean surface reflectivity	SYS	Optimum IFO operation parameters	Specific mirror reflectivity values
Surface reflectivity tolerances		Contrast defect	Coating uniformity
Element surface contamination control (cleaning, handling)	SYS	IFO sensitivity degradation	Lowering of Qs Increased light scatter
		LIGO down time	Damage of optical surfaces

3.2. Characteristics

3.2.1. Performance Characteristics

The discussion of the COC requirements will be broken down into the following characteristic areas:

- Physical Size and Shape.
- Mechanical Q
- Matching to LIGO IFO parameters.
- Wave front distortion
- Light scattering and absorption.
- Diffraction loss.
- Thermal noise and quantum limit.
- 2000 meter IFO.

3.2.1.1 Physical Size and Shape.

Requirements on the COC allow a nominal physical prescription summarized in table 2. This, and subsequent sections aim to justify this prescription in detail. Many alternative prescriptions can be arrived at via differing emphasis on the many requirements. One such alternative is discussed in Appendix L.

3.2.1.1.1 Shape

The exact right circular cylindrical geometry is required to be slightly altered as follows:

- Edges are to be conferred in accordance with standard optical fabrication safety practice (reducing the face diameters by 4-6 mm from the cylindrical diameters).
- Surface 2 on each element will have a wedge angle with respect to the cylindrical axis for ghost beam aiming to suppress the deleterious effects of stray light (SYS requirement) and to facilitate pick-off of signals for servo control (ASC and LSC requirements).
- The ITM, ETM, and RM primary, ER, surfaces have a slight spherical concavity (all secondary (AR) surfaces are taken to be nominally flat).

3.2.1.1.2   Diameter

For TMs the diameter and mirror radii of curvature are selected to minimize TEM_{00} mode diffraction loss (see appendix 1) and thermal noise (see 3.2.1.7). An additional margin of at least 0.6 cm is included to allow for suspension settling, centering tolerance (see 1.5.1.1 and 1.5.1.6), and OSEM clearance. The aspect ratio is then chosen to insure sufficiently high internal mode frequencies and Q. Within these constraints the important practical requirement that the COC be all the same basic size and not too large was imposed.

3.2.1.1.3   Beam Splitter

- For $R_{ETM} = R_{ITM}$ (symmetric arm cavities) the in line cavity beam suffers unacceptable edge clipping loss (~500ppm) traversing a $\phi_s = 25cm$ BS (see Appendix A for details on these losses). The prescription for table 2 was to adjust $R_{ETM} > R_{ITM}$ such that the ETM spot size just fills a $\phi_s = 24cm$ aperture at the 1 ppm level. For the thinnest BS (4cm) deemed suitable for precision optical fabrication, the in line loss then becomes 90 ppm (outline and incident beams suffer ~4ppm clipping).
- Since the beam foot prints on the BS are elliptical, suspension elements (OSEM, magnets) can conveniently be placed away from the major axes with no additional substrate diametrical margin required.
- The thin BS of table 2 will necessitate a specially small wedge angle. A 1° wedge produces a thickness variation of 11% across the full diameter (assumed limit for thermal and mechanical integrity^{TBD})

3.2.1.1.4   End Test Mass

The beam reaches its largest Gaussian radius at this element (4.57 cm). Although this leaves only a ~0.5 cm margin from the 1ppm energy contour to ϕ_s OSEMs and other obstructions can be designed for secondary surface proximity exclusively.

3.2.1.1.5   Input Test Mass

$w_{RM} \sim w_{ITM} = 3.63$ cm, which is small enough to leave a generous margin for OSEMs, etc. In fact a somewhat smaller ITM/RM could be tolerated, allowing a modest reduction in bulk (transmitted beam) absorption/scattering loss (see 3.2.1.4.6).

3.2.1.1.6   Recycling Mirror

The primary RM surface must have a radius $= R_{ITM}/n_{FS} = 14500/1.47 = 9890$ meters. This prescription prevents the recycling cavity from being explicitly unstable (that is, compensates for arm

cavity matching and the ITM lens power).

Table 2: Physical Parameters of 4000m COC

Physical Quantity	Test Mass ETM	Test Mass ITM	Beam splitter	Recycling mirror
Diameter of substrate,ϕ_s (cm)	25	25	25^{TBD}	25
Substrate Thickness, d_s (cm)	10	10	4 **TBD**	10
1 ppm intensity contour diameter (cm)[a]	24	19.1	30.2^b	19.2
Lowest internal mode frequency (kHz)	6.79	6.79	3.58	6.79
Weight of Suspended Component (kg)	10.7	10.7	6.2	10.7
Wedge angle (Surf. 2)^{TBD}	$\leq 3^o$	$\leq 3^o$	$< 1^{oTBD}$	$\leq 3^o$
Nominal surface 1 radius of curvature (m) and g_i factor	7400 g_2=.46	14540 g_1=.725	∞	9891 g=.9984

a. See Appendix A for exact definition.

b. For these 45° angle of incidence optics, this is the smallest diameter circle centered on the optic face which is everywhere outside of the 1 ppm intensity field.

3.2.1.2 Internal resonances, Qs, thermal noise and quantum limit.

3.2.1.2.1 Quantum limit.

What is termed the standard quantum limit for IFO sensitivity depends on the TM's mass. Within the order of magnitude of COC masses of table 2 this sensitivity limit (1.5.2.3) will be less than 1/10 the initial LIGO sensitivity goals. This margin would allow ~100 fold increase in laser power before SQL would dominate LIGO performance with the COC prescibed here. However it is anticipated that the initial COC will be limited by available material quality (see 3.2.1.5) to handling < 10 times the initial power beams.

3.2.1.2.2 Thermal noise

Only the thermal noise of the TM substrates will be considered here since the contribution of the other COC is much less important (this has been explicitly confirmed for the BS of table2: see 1.5.1.3 appendices B and C). The TM internal thermal motion can be modeled as excitation of the substrates internal mechanical modes, so that their influence is controlled via the following mechanical properties, summarized in table 3 and in figure 4 (see also appendix B for discussion of this figure):

3.2.1.2.2.1   Substrate intrinsic Q

A principle reason for the choice of FS for the COC is its known high intrinsic Q. The particular grade and fabrication batch chosen must be carefully monitored to allow internal mechanical mode Qs of $\geq 5 \times 10^6$ (averaged over some suitable range of lowest modes^{TBD}).

3.2.1.2.2.2   Substrate diameter and thickness

These dimensions determine the mode resonance frequency spectrum.The choices of table 2 determine an initial mode sequence listed in table 3, and described in appendix C (for ideal cylindrical shape). Shape perturbations (face wedges, bevels, substrate imperfections) are assumed to not essentially modify the spectrum or Qs.

3.2.1.2.2.3   Attachments and contamination

Any contacting material (coatings, or contamination) or coupling to external systems (SUS) can degrade the intrinsic Qs. A rough budget of such possible effects is in Table 3.

3.2.1.2.3   Servo control interference.

TM thermal noise contribution to $h_{equiv.}$ is only slowly dependent on d_s. It may, however, be practically very difficult to implement servo control loops for the COC with too low internal resonant frequencies (nearer to the loop unity gain frequency). The TM d_s required in table 2 were chosen to keep internal mode resonant frequencies well above control loop unity gain frequencies (~100 Hz). For the BS control loop gain-bandwidth margin required is much less (1.5.16), so that lower internal mode frequencies are tolerable. See appendix C for more discussion.

Table 3: COC Internal Thermal Noise Requirements

Parameter	RM	BS	ITM	ETM	FM
$\nu_0 / \nu_1 / \nu_2$ (kHz)^a	9.42/ 14.3 22.2	5.26/ 14.4 17.8	9.42/ 14.3 22.2	9.42/ 14.3 22.2	9.42/ 14.3 22.2
Q_{avg} minimum of bare substrate x 10^{-6}	.05^{TBD}	> .3	5	5	.3^{TBD}
Effective Q of operational optic x 10^{-6}	.02^{TBD}	.1	2.0	2.0	.15^{TBD}
h_{equiv}@100Hz^b x 10^{-23}	-----	.085	1.26	1.08	.06
h_{equiv}@1kHz^b x 10^{-23}	------	.027	.40	.40	.02

a. First three axisymmetric internal substrate resonances (table 2 sizes)
b. Contribution to IFO strain noise for each optic with parameters of above entries.

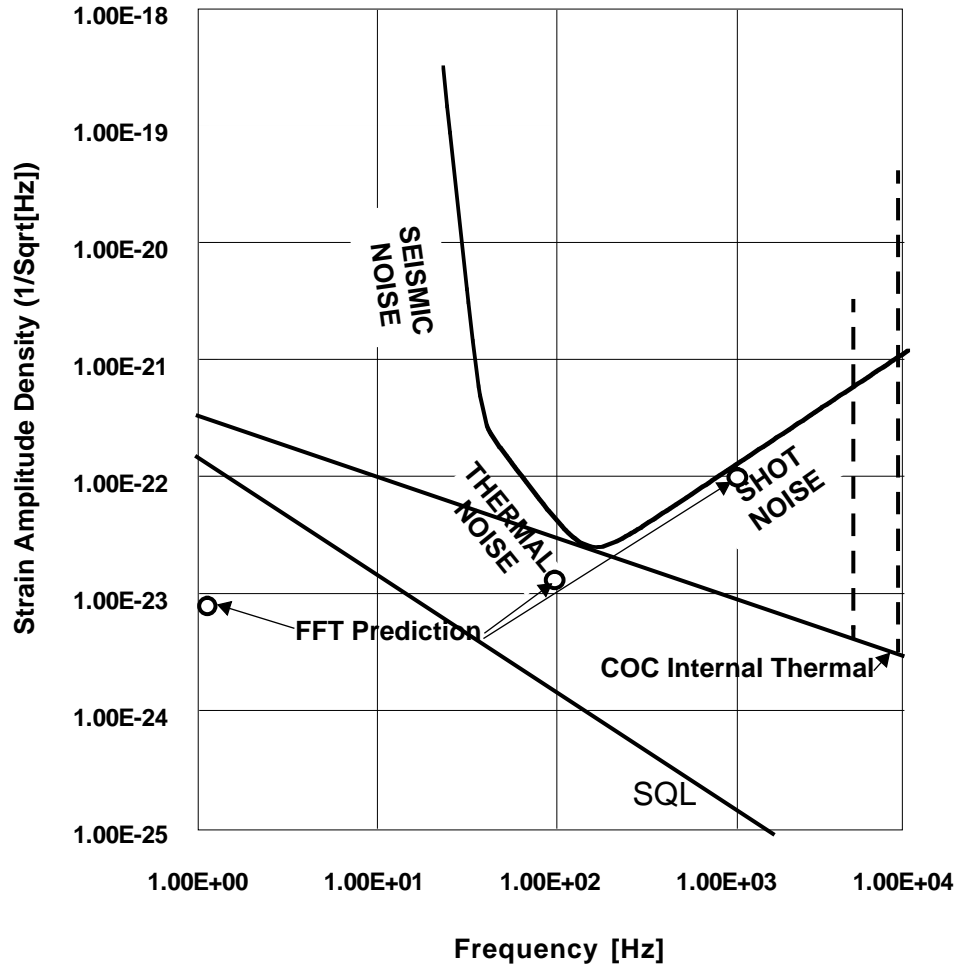## LIGO Initial Interferometer Noise Equivalent Strain

Figure 6: COC Internal thermal contribution to strain noise

3.2.1.3   Matching to SYS IFO parameters

The overall optical design of the IFO depends on the average effective optical characteristic values of each optical surface on which the main beam impinges. Matching of such characteristics between the two IFO arms is also a requirement. In this section we assume that absorption and scattering losses are negligible (justified in light of the expected performance of 3.2.1.5)

3.2.1.3.1   ERITM reflectivity

The SYS arm storage time (4000 m) of $8.8 \; 10^{-4}$ sec. requires the ERITM coating to have T=0.03 ±.003. However the match, $T_{arm \; 1}$ - $T_{arm \; 2}$, is to be within ± 0.0003, the criteria for which are developed in appendix D.1.

3.2.1.3.2   ERRM reflectivity

The current "best educated" 1064 nm FFT model run yields an optimized transmission for the ERRM coating of 0.028. However this depends on imprecisely known parameters, principally the achievable arm cavity mirror surface quality. A tolerance of +.005/-.01 will be required for the ultimately selected transmission value (see appendix D.2).

3.2.1.3.3   ERETM transmission

The ERETM would nominally have unit reflectivity. However a small leakage transmission is desired in order to aid in locking and IFO monitoring. Due to the large intensity build up in the arm cavities (> 10 kWatt) even a 1ppm transmission ($\leq$ anticipated coating absorption) will provide >10 mW for the servo. A different criterion is that the loss due to this residual transmission be small compared with the dominant cavity loss mechanism, which will be the scattering loss determined by the cavity mirror surface quality. This loss may be $\leq$ 25 ppm (per surface). Practical quarter wave stack dielectric mirrors reach a point of diminishing return at $\geq$ 36 layers. At 1064 nm a SiO_2/Ta_2O_5 stack design requires $\geq$ 40 layers for $\leq$ 10 ppm transmission. As will be discussed in 3.2.1.4, excessive stack thickness should be avoided.

3.2.1.3.4   AR coating reflectivity

In order that the ghost beam loss off the recycling cavity AR coated faces (surface 2) be small compared to the arm cavity losses (e.g. in an arm cavity with power gain of ~130 and losses < 50 ppm) their mean reflectivity should be $\leq$ 1000 ppm. This bound will provide adequate signal for control and diagnostics (~100 mW per optic) and allows a coating design whose reflectivity is inherently insensitive to surface position variations coating layers (1.5.1.9).

3.2.1.3.5   ERBS coating

The ERBS coating must perform a beam splitting of 45° incident light (S polarized), such that the exit beams are equal in power within 10% (including the effects of absorption and the ARBS coating). See appendix D.3

3.2.1.3.6   Effective TM curvature radii

With an arm length datum of L =4000m the *effective* TM primary surface curvature radii are required to satisfy $g_1 g_2$ =1/3 (g_i = 1 - L/R_i). With a requirement $|\Delta g_i/g_i|$ <.02 (exact value TBD), we require R_{ETM} =7400 $\pm$ 150m, and R_{ITM}=14540 $\pm$ 290m. Appendix F.1 discusses the requirement (stated in table 4)on the arm to arm match of this effective radius.

3.2.1.4   Wave front distortion

Imperfections in the effective surface profile (which includes the combined influences of the substrate and its coating) and within the FS bulk(index and birefringence inhomogeneities) of the COC optics all contribute to distortion of an ideal TEM_{00} mode wave front propagating in the IFO. Table 4 summarizes required limits to these distortions.

The wave front distortion introduced by non-normal incidence of the beams (including the ~ 45° BS, wedge angles, and residual effective tilts of the real distortions) will be considered a special case: the beam is *deviated* (according to the Fresnel laws) and this will not be considered a

true distortion since it will be allowed for in the basic IFO configuration or can be nulled by servo control. An associated true distortion (astigmatism to lowest order) may be shown to be negligible (LIGO note c 1993, Y. Hefetz and N. Mavalvala) compared to the requirement of 3.2.1.4.5.

In a properly aligned IFO the CD_c will result predominantly from the non TEM_{00} components of the distorted waves. However CD is generally(e.g. table 12) a small fraction ($<$ few x 10^{-3}) of the total carrier IFO loss. Therefore it is only a minor constraint on G_R and the resultant shot noise limit. In this section we assume the value $CD_c \leq 1$ x 10^{-3} (≤ 150 mW dark port power) for the requirement on the contrast defect.

Table 4: Required limits on sources of wave front distortion (surface 1)[a]

Descriptive section	Requirement	Test masses		Beam splitter, Fold mirrors	Recycling mirror
		ITM	ETM		
3.2.1.4.1	Arm-arm match of R_{eff} (fractional)	0.015	0.015	0.015	N/A
3.2.1.4.2	rms surface errors for $w > \lambda_s >$ 2.3 mm out to ~$2w$ diameter[b]	$\lambda/1200$	$\lambda/1200$	$\lambda/200^{TBD}$	$\lambda/200^{TBD}$
3.2.1.4.3	rms surface errors for $2w > \lambda_s >$ 2.3 mm past $2w$ diameter[b]	$\lambda/600$	$\lambda/600$	$\lambda/100^{TBD}$	$\lambda/100^{TBD}$
3.2.1.4.4	rms surface error for 2.3mm $> \lambda_s >$ 1.3μm out to ~ $3w$ diameter	<0.4 nm	<0.4 nm	$<.8$ nm	$< .8$ nm
3.2.1.4.5	rms surface errors for $\lambda_s > 3$-$4w$	$\lambda/160$	$\lambda/160$	$\lambda/320^c$	$\lambda/160$
3.2.1.4.6	rms transmission OPD for $2w > \lambda_s$ > 2.3 mm out to ~ $2w$ diameter[b]	$\lambda/50$	N/A ($\lambda/20^{TBD}$)	$\lambda/100$	$\lambda/50$
3.2.1.4.7	Birefringence (transmission) δ (mrad)	20	N/A	< 10	< 50

a. all wavelengths are interferometer beam laser wavelengths
b. Measured after removal of surface wave components longer than requirement λ_s band limit
c. BS only

3.2.1.4.1   *Effective radius of curvature*

As a typical example consider the arm cavity forming mirrors. The input laser beam (IOO) may be matched equally into both arms if the mirror spacings and effective curvatures are identical. If not, only a mean matching can be achieved. The R_{eff} matching tolerances in table 4 limit the curvature mismatch contribution to CD to $\leq 2.5 \; 10^{-4}$. Derivation of this is discussed in appendix F.

VIRGO advocates (VIRGO final design v1.0) a strategy which obviates so tight a tolerance on R_{eff}. Both arms, even with mismatched R_{eff}, can be matched if their relative lengths are free to be adjusted.

3.2.1.4.2   Mid λ_s central errors

These are the imperfections which the 86% energy foot print of the beam sees. They produce approximately this proportion of the cavities' diffractive loss. The specific requirement values are derived from FFT modeling results. Plausible mirror imperfection maps are represented in the model. The integrated rms scale of imperfection is varied and the scale at which $G_R \geq 30$ occurs is chosen. Other model parameters are taken to be close to those elsewhere in this document (3.2.1.4.1,.4.4,.5.3,.5.1,.1.2). The modeling so far is *preliminary* and has *not* been fine tuned, especially with respect to arm to arm balance of optical properties[TBD]. See appendix G for detail.

3.2.1.4.3   Mid λ_s peripheral errors

Only 14% of the beam energy lies outside of $\phi_s = w$. It is therefore expected that surface imperfections in this periphery will contribute much less to diffractive loss from the TEM_{00} beam. This is born out by FFT modeling which is the basis for the requirement values. FFT runs with mirror parameters at least as good as those of table 4 were compared, where the mirror errors beyond 2-3 w_{ETM} were allowed to scale. For peripheral errors scaled up ~ 3x the quantities G_R, and h(DC) or 100Hz) degraded less than 5% (this analysis is preliminary, e.g.[TBD] at 1064nm).

3.2.1.4.4   Micro-roughness

 In order to reduce the requirement for all short λ_s (cutoff = 2.3mm) imperfections to a single rms value, some reasonable assumptions (appendix H) are needed, based on the condition $\lambda_{s,cutoff} <<$ 2w. So defined, the micro-roughness merely parameterizes the diffuse scatter loss, which, at 1064 nm, is 22 ppm/surface for micro-roughness rms = 0.4nm (appendix H). While micro-roughness measures a physical surface topography, we are concerned with net reflected phase front distortion. However, by stating the micro-roughness requirement explicitly in terms of loss (in 3.2.1.5.3), there will be no ambiguity (and evidence, appendix H, indicates that coatings of the quality anticipated do not degrade this effective surface rms).

The very long arm length cavities are effective spatial filters rejecting diffuse scatter contribution to $CD_c < 10$ ppm. This does not necessarily hold for recycling cavity elements[TBD](see appendix J) where a substantial fraction of their diffuse loss may channel out the dark port. Allowing $CD_c \leq 10^{-4}$ from this as an upper limit drives the non-arm cavity values in table 4 (but not the net loss requirement of table 5, 3.2.1.5.3).

3.2.1.4.5   Long λ_s errors.

For surface error Fourier components of $\lambda_s \geq 4w$, one anticipates only a contribution to beam matching effects (as taken into account by 3.2.1.4.1). This is because sines and cosines of periods $\geq 4w$ are very good approximations to planes and paraboloids respectively, over a central half wave span (representing most beam energy). Plane contributions are tilt effects removed by ASC control. Paraboloids effect the axisymmetric mode matching and are part of the consideration of

3.2.1.4.1. In general the Fourier decomposition is two-dimensional so that a matching between dimensions (astigmatism requirement) is inferred (and included in the rms requirement).

The BS carries a tighter requirement since wave front curvature generated by reflection off it is *additive* between the arms. That is, an *intrinsic* mismatch is created by splitting surface curvature in this element.

3.2.1.4.6   *Transmission OPD errors*

Transmission distortion occurs only outside of the arm cavities so that it does not factor strongly into G_R degradation. For on-resonance arm cavities the net distortion of the carrier wave front returning from each arm is suppressed (see appendix I). This is substantiated by FFT modeling which shows no CD_c introduced by ITM OPD errors at least at the level of the table 4 entry. In contrast, the side band wave fronts have a substantial, if not dominant, distortion from ITM (double pass) and BS transmission (which, however, has essentially no effect on the net IFO strain sensitivity in the context of the *entirely static* FFT model).

For the BS such a carrier wave front error suppression is not so evident[TBD]. Hence a tighter requirement is set. FFT modeling of BS substrate OPD errors at the same level as used for the ITM also show negligible degradation in CD_c. Further modeling and analysis is needed to confirm this.

3.2.1.4.7   *Birefringence Effects*

Birefringence effects have been considered by Winkler, et al (1.5.2.3). These may be: intrinsic, heating strain induced, or mechanical stress induced. We place a nominal requirement on intrinsic material birefringence, however the thermally induced effects are expected to dominate by a large margin.

3.2.1.5   **Scattering and absorption**

It is convenient to define a category of IFO cavity loss due to absorption and scattering. Absorption is assumed to be uniform across the surface and to be linear (a good approximation for the low fractional values anticipated). Scattering here is categorized to mean that resulting from local surface "micro-roughness" imperfections (see appendix I.3). The surface scale for onset of this regime is taken to be 2.3 mm (corresponding to the break between sections 3.2.1.4.3 and3.2.1.4.4). This is somewhat arbitrary (and the results are believed to be insensitive to it) but corresponds 1) to the limit where the FFT modeling programs used to describe the IFO can follow the effects of imperfections diffractively, and 2) the scale where imperfections and the loss they generate can reasonably be presumed to be uniform and thus can be modeled as a lumped param-

eter loss along with the absorption.

Table 5: Specified limits to scattering and absorption (in ppm) by COC optics[a]

Section reference	Loss Source	input TM	end TM	BS & Fold mirrors	Recyclin g Mirror
3.2.1.5.1	Bulk scattering of transmitted beams	$<50^{TBD}$	N/A^{TBD}	$< 50^{TBD}$	$< 50^{TBD}$
3.2.1.5.2	Total surface absorption Surface 1	< 2	< 4	<50	< 50
3.2.1.5.3	Surface scattering from effective mirror micro-roughness	<50	<50	<100	<200
3.2.1.5.4	Ghost beam loss (surface 2 origin)	~600	N/A	~100	~1000
3.2.1.5.5	Accumulated contamination scattering + absorption	< 1	< 2	<30	< 30
3.2.1.5.6	Bulk absorption within substrate	< 40	N/A	<20	<40

a. All entries are per mirror, single reflection or single pass.

3.2.1.5.1   Bulk scattering

It is assumed that this category of loss does not contribute to substrate heating. The requirement value is chosen to make this contribution to loss much smaller than that from other mechanisms. Expected scattering loss from high homogeneity FS is much less (< 2ppm/ cm or <16 ppm for the ITM)

3.2.1.5.2   Surface absorption

Very low fractional surface absorption is required of the arm cavity coatings due to consequent thermal distortions. An analysis (1.5.2.4, and see 3.2.1.7.3) of the change in R_{eff} of a surface due to thermal distortion was used. Using the same criterion as 3.2.1.4.1 of table 4 one finds that ~ 3 ppm surface absorption on one (only) ERITM would produce the same mismatch. (exactly matched absorptions between arms would ameliorate this effect but this worst, unmatched case is used for the requirement here).

3.2.1.5.3   Surface scattering

Operationally this includes all non-absorptive loss at the IFO surfaces, which cannot be explicitly accounted for by diffraction modeling (e.g. the FFT wave front code). FFT model analysis shows that values of this loss of up to ~100 ppm per arm cavity surface can be tolerated to maintain $G_R \geq$ 30. However this requires mirror surface errors to be even better than those required in 3.2.1.4.2-3. Direct estimates of this loss (see appendix H) based on the reasonable requirement 3.2.1.4.4 indicate that ≤ 25 ppm should be possible for even non superpolished surfaces. The required value of table 5 is chosen to accommodate the table 4 requirements but also leave a margin for uncertainty in actual scattering performance.

3.2.1.5.4   Ghost beams

Here the transmission residual beam through the ERETM is *not* included (see 3.2.1.3.3). Then all other ghost reflections are recycling cavity losses. Single ghost losses ≥1000ppm become comparable to contrast defect and to *total* absorption and surface scatter loses. The table 5 values are required to keep this balance. Although AR coatings could be obtained to limit reflection to ~ 50 ppm, the resultant ghost wave fronts would have poor phase stability (1.5.1.9). The requirement allows coating design to avoid this. Since ghost beams will be used for length control pick-off a significant^{TBD} detectable signal is required (≥ 100 mW for table 5 values). For beams transiting the AR coatings a full analysis shows that there is no similar sensitivity to coating uniformity variation. It would therefore be permissible to use minimum reflectance AR coatings e.g. on the BS (does not supply control signals) where uncontrolled beam loss is a possible problem (1.5.1.6).

3.2.1.5.5   Contamination loss

This requirement derives from 3.2.1.5.2: any *acquired* surface loss should be substantially less than that intrinsically desired. A time scale needs to be attached to such accumulation^{TBD}(see 3.2.4 and 3.2.5).

3.2.1.5.6   Bulk absorption

For available FS, direct absorption loss is not a dominate concern. However "thermal lensing' due to bulk absorption is, and drives the values of table 5. The ITM requirement is for specific absorption <5 ppm/cm which is very demanding. The associated lensing produces $CD_c \geq 10^{-3}$. Thus the entire CD_c budget may be dominated by this effect if not balanced between arms (see appendix I). The effect of BS lensing is intrinsically unbalanced, hence the higher set requirement.

3.2.1.6   Diffractive (aperture) loss.

Each COC presents a finite aperture to the cavity laser beams which will cause diffraction loss. Choosing the good optical apertures reasonably large (radius $3w$) assures negligible TEM_{00} diffractive loss. Here we assume the beams are centered on optics, and idealized effective optical apertures, ϕ_e (normalized to w) ≤ ϕ_s, are considered for each COC. A full analysis for choosing ϕ_e is complex^{TBD}and partial work toward it based on FFT modeling, and the criteria to follow is summarized in table 6.

Table 6: COC Diffraction Loss Requirement

Parameter	*RM*	*BS^a*	*ITM*	*ETM*	*FM*
w (cm)	3.64	5.15	3.63	4.57	3.64^{TBD}
ϕ_e (w)^{TBD}	4.6	5.0	6.0	5.3	6.0
diffractive loss ^{TBD}	40 ppm	<100 ppm	<.3 ppm	~ 1ppm	<.3 ppm

a. For BS and FM assume a circumscribing circle.

3.2.1.6.1   Static loss budget

If the IFO is exactly static (as the FFT model treats it) the requirement would simply be to minimize absolute diffractive loss. FFT modeling has concentrated on cases where ϕ_e is $\geq$ the 1 ppm TEM_{00} energy foot print. Therefore direct diffractive loss is considered negligible. Indirectly a substantial fraction of IO power (up to ~50%) is lost to diffraction of distortion exited higher transverse modes (HTM). Since the excitation is proportion to TEM_{00} power, the arm cavities dominate this fraction. With large enough arm cavity ϕ_e the HTM energy would remain in the arm cavities and mostly dissipate as a negligible CD_c loss (~ $50\%/T_{ETM}$). This trade-off (between CD_c and total diffractive loss) is evident in FFT runs over ϕ_e (see table 12, appendix K). However the trend to larger G_R with ϕ_e is weak over a range of reasonable ϕ_e when full models with competing losses and constraints are considered.

3.2.1.6.2   Dynamic stability and phase noise

In a real IFO the scattering coefficients for generating HTMs are time (noise) dependent. The IFO is quiet so that the overall power loss balance discussed above will hardly be modulated. However a kaleidoscopic HTM mix in both the CD_c and CD_{sb} will induce a phase changing GW noise. An extreme case (but simply modeled: appendix K.3) is an individual, nearly degenerate, parasitic HTM with some parametric coupling to the TEM_{00} mode. The relatively large 40 meter ϕ_e support a resultant instability. The table 6 requirements $\phi_e(w)$ address this noise based on the following criteria;

- FFT modeling shows CD_c to be almost entirely contributed by HTMs, so that, in general, modal noise in the GW signal is avoided by minimizing CD_c. Table 11 (appendix K) shows that HTMs can be strongly filtered with respect to the TEM_{00} by finite apertures. Thus one could expect reduced CD_c with smaller ϕ_e until the TEM_{00} is itself encroached upon. Preliminary FFT study of CD_c as a function of ϕ_e (table 12) indeed show a shallow CD_c minimum at ϕ_e= 5-6 (ETM scaling). This is taken as the ETM requirement.
- Smaller ϕ_e not only erodes the TEM_{00} power budget (the normalization of CD_c)but also establishes a source of HTM by edge diffraction which is sensitive to beam position relative to the mirror faces. Appendix K.1 presents an analysis indicating that this source cannot be a problem for $\phi_{e,ETM} \geq 4.8$ (~ 10 ppm loss contour).
- For the g_1g_2= 1/3 arm cavities the few HTMs with lower diffraction loss at $\phi_e \leq 6$ are all suppressed by being far off resonance. This is not the case in the recycling cavity. In this degenerate cavity it may be desirable to impose stronger HTM diffractive loss by optic apodization. FFT studies of CD_c and CD_{sb} vs $\phi_{e,RM}$ (for example) will quantify this as a requirement[TBD]. Table 6 takes the RM to be the limiting aperture in this sense with an estimated value.

3.2.1.7   Basic parameters of 2000 meter IFO.

Here the COC for a half arm cavity length (= 2000m) IFO is described whose design are assumed to be as closely analogous as possible to the full length IFO considered elsewhere in this document. The assumptions of 2.4 and 2.5 hold with the differences:

- Several arm cavity beam geometries (including Flat/Curved) would fit within the constraint

of ϕ_s= 25cm. Symmetric Curved/Curved is chosen primarily to minimize beam intensity at the TM primary coatings (see3.2.1.7.2). Then $g_{1,2}$= $3^{-1/2}$ and R_{eff}= 4732m. Note that is not possible to choose 4000m IFO TM mirror curvatures to simultaneously satisfy the 2000m IFO in a way which would reduce overall COC types count.

* This geometry specifies that w = 2.88 cm on the TM primary surfaces.
* To utilize the same arm vacuum enclosures the half length IFO needs ~45° incidence fold mirrors between beam splitter and ITM (see figure 2).

With these variant parameters most of the requirements for the COC remain unchanged from those described in the previous sections. Only differences will be discussed.

3.2.1.7.1 COC sizes- thermal noise

With smaller waist diameter the half length IFO beams could be accommodated with the smaller COC sizes. However the considerable advantage of using optics identical (except for some surface curvatures) to those in the 4000m IFO motivates the proposed choices. The most significant result of this choice is that the displacement noise from TM internal thermal noise increases. This is due to the fact that the coupling of TM thermal noise to the cavity beam is weighted toward the optic face center. Smaller w beams are thus more effected. The rms thermal displacement noise for each arm cavity is 3.7×10^{-20}m/Hz$^{1/2}$ which is 25% larger than that in the 4000m cavities.

Table 7: Physical Parameters of 2000m COC

Physical Quantity	Test Mass ITM	Test Mass ETM	Beam splitter	Recycling mirror	Folding mirrors
Diameter of substrate (cm)	25	25	25^{TBD}	25	25
Substrate Thickness (cm)	10	10	4 **TBD**	10^{TBD}	10 cm
1 ppm intensity contour diameter (cm)[a]	15.1	15.1	23.6[b]	15.2	21.4[b]
Lowest internal mode frequency (kHz)	6.79	6.79	3.58	6.79	6.79
Weight of Suspended Component (kg)	10.7	10.7	6.2	10.7	10.7
Wedge angle (Surf. 2)^{TBD}	≤3°	≤ 3°	≤ 1°	≤ 3°	≤ 3°
Nominal surface 1 radius of curvature (m)	4732	4732	∞	3219	∞

a. See Appendix 1 for exact definition.

b. For these 45° angle of incidence optics, this is the smallest diameter circle centered on the optic face which is everywhere outside of the 1 ppm intensity field.

3.2.1.7.2 SYS IFO parameters

- The 2000m arm storage time will remain 8.8 x 10^{-4} Sec. This requires T = 0.015 for the ERITM coatings.
- To ameliorate increased arm cavity losses (see 3.2.1.3.3 and the next section) a higher ERETM reflectivity may be necessary[TBD]. This would require a larger ER dielectric mirror stack layer number design (> 40 layers).

3.2.1.7.3 Arm mirror surface quality

Because of the parameterization of 3.2.1.7.2 the power in the arms will be twice that in the full length IFO and the intensity on mirror surfaces will be 3.20 times that at the highest intensity surface(ETITM) in the 4000m IFO (if Flat/Curve were chosen for the 2000m IFO this factor would be 5.54!). This has the following consequences for the arm mirror surface quality:

- The absolute arm cavity diffractive losses due to cavity mirror surface errors (3.2.1.4.2-4) will be ~ twice as large as for the 4000m IFO if G_R~ 30 is maintained. For fixed IO laser power, G_R~30 can only be maintained if the rms surface error requirements are tightened. To some extent this will happen naturally since the smaller beam waist will impinge within a smaller central (less rms error) surface area.
- A similar tightening of the surface scatter (3.2.1.5.3, and 3.2.1.4.4) requirements will occur. A requirement in the range of 20-30 ppm micro-roughness scatter per surface may be necessary.The best blend of surface figure and scattering required for maintaining G_R>30 is TBD.
- Coating thermal absorption becomes a much more serious problem. The requirement of table 5 (line 2) for the ITM is no longer tight enough. The thermal distortion due to a four fold surface intensity increase (using $1/R_{eff} = (\alpha\, P_{cavity}\, L_{coating})/(2\pi\, \kappa\, w^2)$ where α is the thermal expansion coefficient and κ is the thermal conductivity) is almost twice the table 5 optical requirement. Sub ppm surface absorption will be required[TBD].
- Requirements on the surface contamination (table 5 line 5) will similarly become more stringent[TBD].

3.2.2.   Interface Definitions

The naming convention for COC is contained in 1.3.1 and figures 1and 2.

3.2.2.1   Interfaces to other LIGO detector subsystems

3.2.2.1.1   Mechanical Interfaces

The Core Optics Components have mechanical interfaces with other subsystems as shown in table 8 (Fig. 1, 2, and 7). It should be noted that with the possible exception of an electrostatic shield coating applied to the COCs, and the influence of out gassing, all mechanical interfacing items belong to the SUS subsystem.

Table 8: Mechanical interfaces between COC and other Detector subsystems

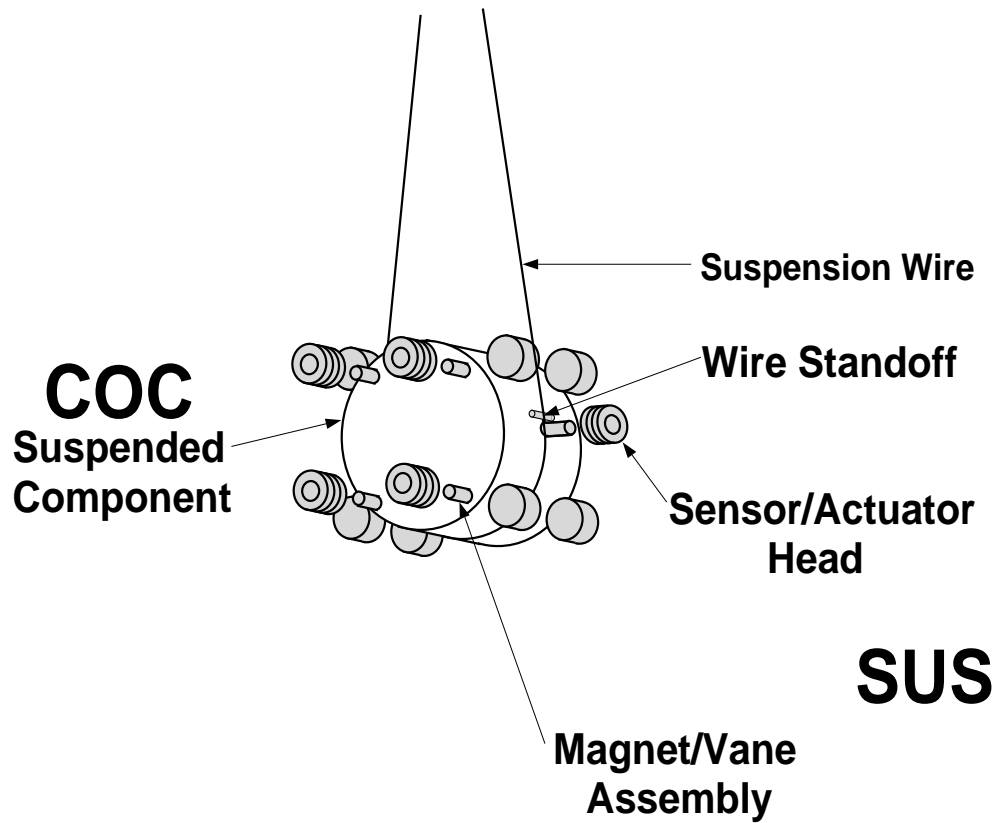| Mechanical Interfacing Points			Drawing/ Doc#
COC Element/ Surface	*Other Subsystem Element*	*Contact/Connection method*	
All Elements/ Cylindrical side	SUS-Suspension wire	Constrained slip fit	
All Elements/ Cylindrical side	SUS-Wire standoff	Adhesive	
All Elements/ Cylindrical side & Surface 1 or 2	SUS-Magnet/Vane assembly	Adhesive	
All Elements TBD/ Cylindrical side	TBD-Electrostatic contact	Electrostatic shield coating TBD	
All Elements/All surfaces	All Subsystems Surfaces	Out gassing from all elements	
Critical Dimension/Size			*Drawing/ Doc#*
Offset of COC element optical axis relative to the top surface of the HAM Optics platform (= d_1 in SEI DRD). Offset of COC element optical axis relative to the bottom surface of the BSC Optics platform (=d_2 in SEI DRD			

COC
Suspended
Component

Suspension Wire

Wire Standoff

Sensor/Actuator Head

SUS

Magnet/Vane Assembly

Figure 7: Mechanical interfaces of COCs

3.2.2.1.2   Optical interfaces

Optical interfaces are represented in figure 8. The optical interfaces to the COC may be divided into two categories:

- Primary IFO beams received from(IO) and delivered to(OO) the COC subsystem from the IOO subsystem. These beams are to have vertical polarization, to within $\pm 1^o$ TBD, with respect to the plane defined by the two IFO arms.
- Diagnostic beams which interface to the ASC subsystem and are either input to COC from the ASC or derivative from the primary IFO beams (e.g. ghost beams off wedged AR surfaces).
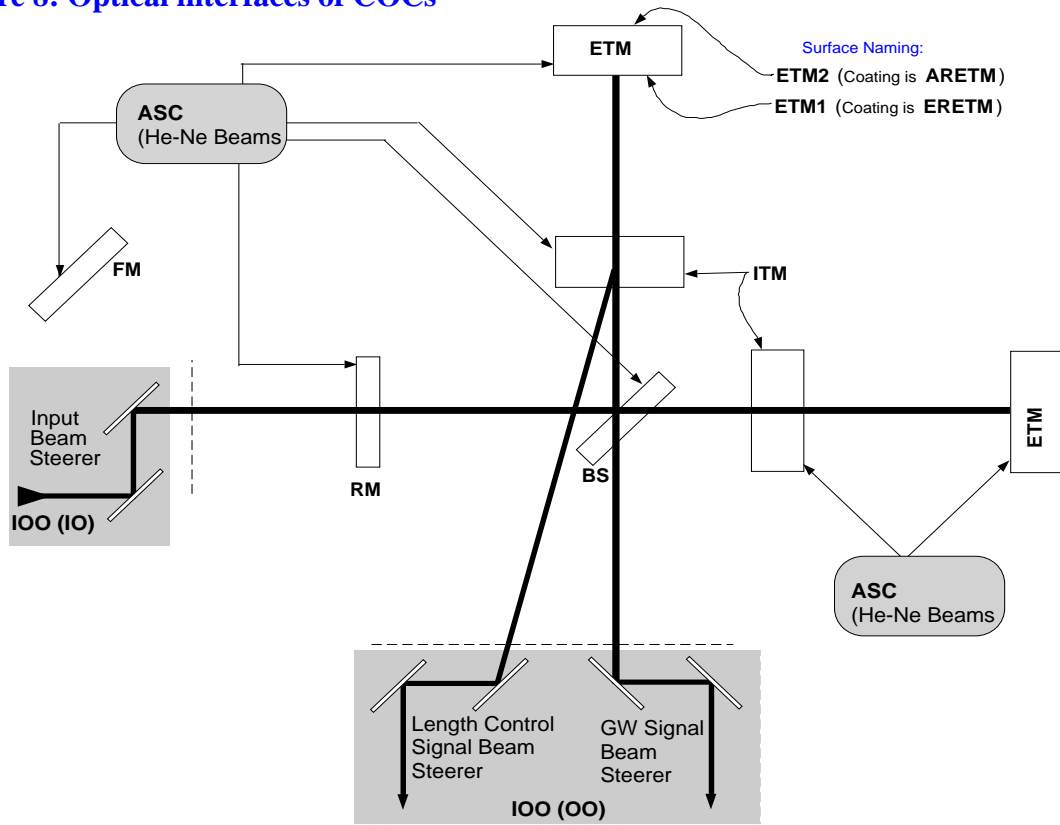
Figure 8: Optical interfaces of COCs

Table 9: Optical interfaces between COC and other Detector subsystems

COC Element/ Interface	Other Subsystem	Interface & Characteristics	Drawing/ Doc.#
Recycling mirror (RM) secondary surface	IO output steering mirror	Laser power Laser Beam size	
BS secondary surface	OO GW signal input steering mirror	Beam power Beam size	
ITM secondary and second surface of primary	OO length control signal input steering mirror	pickoff light power fraction	
All COC secondary surfaces.	ASC-Beam centering monitor	Ghost beam pickoff AR coating reflectivity	
All COC secondary surfaces TBD	ASC-Optilever beam centering	Auxiliary probe laser beams	

3.2.2.1.3   External interfaces.

The COCs are directly coupled (as compared to being indirectly coupled via the SUS subsystem) to the FAC/VE systems via their vacuum environment. The vacuum system is required to be of a quality such that the integral contamination to the COC surfaces over ~year time scale does not degrade the IFO performance.

3.2.2.1.4   Stay Clear Zones

To maintain the good optical performance required of the COC optical faces it will be necessary to maintain a stay clear cone whose vertex is on the optical axis and whose surface intersects the ~ 1ppm contour of the Gaussian beam intensity at any mirror face. This prescription is to include a ~ 5mm margin for imperfect alignment and suspension settling. Intrusion within these [cylindrically symmetric] cones can be tolerated as long as the intruders for one face "clip" geometrically no more than ~ 1ppm of the impinging beam intensity.

3.2.2.2   Interfaces external to LIGO detector subsystems

3.2.2.2.1   Mechanical Interfaces

None anticipated

3.2.2.2.2   Electrical Interfaces

None anticipated

3.2.2.2.3   Stay Clear Zones

None anticipated

3.2.3.   Reliability

- It is expected that the COC have no inherent hard failure mechanisms. Reliability will be essentially dependent on the extent that they remain free of contamination from external sources.
- An adequate protocol for handling, storing, cleaning, and working around the COC elements must be formulated and assured in practice to avoid breakage or degradation of the optical surfaces. It is to be noted that a single inadvertent scratch on a coated surface will likely constitute breakage.

3.2.4.   Maintainability

It will not be possible to "repair" COC elements. The only form of maintenance will be in cleaning the optical surfaces. There is no inherent contamination mode so that a MTTR for cleaning will not be a requirement imposed on the COC.

- It will be required that effective cleaning procedures for the specific COC materials (fused silica and the optical thin film coating materials) be developed which can be invoked to clean the surfaces when they are determined to be contaminated.
- Tests (e.g. in-situ ring down, ellipsometry, etc.) must be developed to unambiguously signal

contamination since in-situ cleaning or change out of COC elements will cause major LIGO down time.
- Given the COC operational environment (UHV) it is anticipated that the only mechanism for dealing with contaminated elements will be to change them out. However every effort will be made to investigate and develop possible in situ cleaning procedures.

A "ready" contamination test procedure will be implemented on each COC element immediately prior to final (prior to system evacuation) installation in the IFO chambers to certify its initial operational state.

- Consistent with the on time requirements of a LIGO interferometer at the nominal initial LIGO strain sensitivity, is that contamination equivalent to that in table 5 not accrue in less than 2 months operating time. This estimate is based on the assumption that replacing or cleaning the contaminated mirrors will cost an effective observation down time of one month.

3.2.5.   Environmental Conditions

COC elements must be exposed at all times to only the cleanliest possible environments.

- For storage and transport, individual, specially designed hermetic containers will be provided which assure an environment of at least a Class10 clean room environment.
- For open handling, transfer to the IFO chambers, cleaning, and auxiliary examination or testing the elements will be at no times exposed to worse than a Class 100 clean room environment.

The cleanliness requirement for the COC is particularly critical, since first, contamination can lead to *cumulative* irreversible degradation of the optical performance and hence extremely small detectable amount is of concern. Second, cleanliness of the entire LIGO vacuum environment is specified by its impact on the COC, so that all other subsystems are in turn specified in this respect by the COC requirements

.

3.2.5.1   Natural Environment

3.2.5.1.1   Temperature and Humidity

Table 10: Environmental Performance Characteristics (COC)

Operating	*Non-operating (storage)*	*Transport*
+0 C to +50 C, 0-90%RH	-10 C to +150 C, 0-90% RH	-10 C to +70 C, 0-90% RH

3.2.5.1.2   Atmospheric Pressure

3.2.5.1.3   Seismic Disturbance

3.2.5.2   Induced Environment

Certain materials shall not be put in close proximity of the optical surfaces for extended periods of time (even short term placement is to be checked with cognizant optical engineer)

- Synthetic rubber products

3.2.5.2.1 *Electromagnetic Radiation*

 All COC Coatings are extremely sensitive to UV radiation. Severe, non-reversible damage to the coatings can occur with even short term exposure to UV sources. UV sources include direct exposure to welding flash, UV curing lamps, high UV output lamps, UV lasers/markers, plasma discharges, intense direct sunlight, etc. Consult the appropriate optical engineering staff before an potential exposure.

3.2.5.2.2 *Acoustic*

3.2.5.2.3 *Mechanical Vibration*

3.2.6. Transportability

All items shall be transportable by commercial carrier without degradation in performance. As necessary, provisions shall be made for measuring and controlling environmental conditions (temperature and accelerations) during transport and handling. Special shipping containers, shipping and handling mechanical restraints, and shock isolation shall be utilized to prevent damage. All containers shall be movable for forklift. All items over 100 lbs. which must be moved into place within LIGO buildings shall have appropriate lifting eyes and mechanical strength to be lifted by cranes.

3.3. Design and Construction

Minimum or essential requirements that are not controlled by performance characteristics, interfaces, or referenced documents. This can include design standards, requirements governing the use or selection of materials, parts and processes, interchangeability requirements, safety requirements, etc.

3.3.1. Materials and Processes

Such items as units of measure to be used (English, Metric) should be listed and any other general items, such as standard polishing procedures and processes.

3.3.1.1 Finishes

Examples:

- Ambient Environment: Surface-to-surface contact between dissimilar metals shall be controlled in accordance with the best available practices for corrosion prevention and control.
- *External surfaces: External surfaces requiring protection shall be painted purple or otherwise protected in a manner to be approved.*

3.3.1.2 Materials

Requirements for materials to be used, such as out gas properties, corrosion resistance, etc. Should also reference TBD documents on LIGO Materials Standards for Vacuum and LIGO Vacuum Cleaning Standards.

3.3.1.3   Processes

List all LIGO standard processes (as appropriate) for cleaning, coating, polishing, etc.

3.3.2.   Component Naming

All components shall identified using the LIGO Detector Naming Convention (document TBD). This shall include identification physically on components, in all drawings and in all related documentation.

3.3.3.   Workmanship

Standard of workmanship desired, uniformity, freedom from defects and general appearance of the finished product.

3.3.4.   Interchangeability

Specify the level at which components shall be interchangeable or replaceable.

3.3.5.   Safety

This item shall meet all applicable NSF and other Federal safety regulations, plus those applicable State, Local and LIGO safety requirements. A hazard/risk analysis shall be conducted in accordance with guidelines set forth in the <u>LIGO Project System Safety Management Plan</u> LIGO-M950046-F, section 3.3.2.

3.3.6.   Human Engineering

Note: For most detector subsystems, this is not applicable. This is important for CDS, however.

Specify any special or unique requirements, e.g., constraints on allocation of functions to personnel, and communications and personnel/equipment interactions. Also include any specified areas, stations, or equipment that require concentrated human engineering attention due to the sensitivity of the operation, i.e. those areas where the effects of human error would be particularly serious.

3.4.   Documentation

Requirements for documentation of the design, including types of documents, such as operator manuals, etc.

3.4.1.   Specifications

List any additional specifications to be provided during the course of design and development, such as Interface Control Documents (ICD) and any lower level specifications to be developed.

3.4.2.   Design Documents

Refer to the COC Conceptual Design Document accompanying this DRD.

3.4.3.   Engineering Drawings and Associated Lists

Any drawings to be provided and any standard formats that they must comply with, such as shall use LIGO drawing numbering system, be drawn using LIGO Drawing Preparation Standards, etc.

3.4.4.   Technical Manuals and Procedures

3.4.4.1   Procedures

Procedures shall be provided for, at minimum,

- *Initial installation and setup of equipment*
- *Normal operation of equipment*
- *Cleaning processes*
- *Measurement procedures for contamination measurement.*

3.4.4.2   Manuals

Any manuals to be provided, such as operator's manual, etc.

3.4.5.   Documentation Numbering

All documents shall be numbered and identified in accordance with the LIGO documentation control numbering system LIGO document TBD

3.4.6.   Test Plans and Procedures

All test plans and procedures shall be developed in accordance with the LIGO Test Plan Guidelines, LIGO document TBD.

3.5. Logistics

The design shall include a list of all recommended spare parts and special test equipment required.

3.6. Precedence

The following lists the principle COC requirements in decending order of importance

- Primary optical surface quality requirement (both substrate polish and coatings)
- Substrate material homogeneity for primary beam transmitting elements
- Cleanliness requirements
- Mechanical Q requirements
- Physical dimension tolerance requirements.

3.7. Qualification

- Acceptance of the COC elements from the optical fabricator and the thin film coating provider will be subject to a full array of tests which will assure that the requirements of section 3.2.1

above have been met. These tests will be partially conducted by verified tests conducted by the vendors and subsequently completed and supplemented by LIGO "in house" tests.

• As described in 3.2.5 final "ready" cleanliness qualification of COC elements will be conducted by specific tests which can be performed immediately prior to sealing of the elements into their operational vacuum chamber locations

4 QUALITY ASSURANCE PROVISIONS

This section includes all of the examinations and tests to be performed in order to ascertain the product, material or process to be developed or offered for acceptance conforms to the requirements in section 3.

4.1. General

This should outline the general test and inspection philosophy, including all phases of development.

4.1.1. Responsibility for Tests

The COC task leader and designated Detector group personnel will be responsible for all tests, their documentation and interpretation.

4.1.2. Special Tests

4.1.2.1 Engineering Tests

• Absorption test of HR coated surfaces @ 1.06 microns.
• Scattering test of AR and HR coated surfaces to determine net normal incident 1.06 micron light scattered from specular.
• Q measurement of characteristic internal substrate resonance modes
• Interferometric mapping of the optical surfaces.
• Inspection, ellipsometry, etc ^{TBD} to determine the state of optical surface contamination.

4.1.2.2 Reliability Testing

Reliability evaluation/development tests shall be conducted on items with limited reliability history that will have a significant impact upon the operational availability of the system.

4.1.3. Configuration Management

Configuration control of specifications and designs shall be in accordance with the LIGO Detector Implementation Plan.

4.2. Quality conformance inspections

Design and performance requirements identified in this specification and referenced specifications shall be verified by inspection, analysis, demonstration, similarity, test or a combination

thereof per the Verification Matrix, Appendix 1 (See example in Appendix). Verification method selection shall be specified by individual specifications, and documented by appropriate test and evaluation plans and procedures. Verification of compliance to the requirements of this and subsequent specifications may be accomplished by the following methods or combination of methods:

4.2.1.   Inspections

Inspection shall be used to determine conformity with requirements that are neither functional nor qualitative; for example, identification marks.

4.2.2.   Analysis

Analysis may be used for determination of qualitative and quantitative properties and performance of an item by study, calculation and modeling.

4.2.3.   Demonstration

Demonstration may be used for determination of qualitative properties and performance of an item and is accomplished by observation. Verification of an item by this method would be accomplished by using the item for the designated design purpose and would require no special test for final proof of performance.

4.2.4.   Similarity

Similarity analysis may be used in lieu of tests when a determination can be made that an item is similar or identical in design to another item that has been previously certified to equivalent or more stringent criteria. Qualification by similarity is subject to Detector management approval.

4.2.5.   Test

Test may be used for the determination of quantitative properties and performance of an item by technical means, such as, the use of external resources, such as voltmeters, recorders, and any test equipment necessary for measuring performance. Test equipment used shall be calibrated to the manufacture's specifications and shall have a calibration sticker showing the current calibration status.

5   PREPARATION FOR DELIVERY

Packaging and marking of equipment for delivery shall be in accordance with the Packaging and Marking procedures specified herein.

5.1. Preparation

Equipment shall be appropriately prepared. For example, vacuum components shall be prepared to prevent contamination.

5.2. Packaging

Procedures for packaging shall ensure cleaning, drying, and preservation methods adequate to prevent deterioration, appropriate protective wrapping, adequate package cushioning, and proper containers. Proper protection shall be provided for shipping loads and environmental stress during transportation, hauling and storage.

5.3. Marking

Appropriate identification of the product, both on packages and shipping containers; all markings necessary for delivery and for storage, if applicable; all markings required by regulations, statutes, and common carriers; and all markings necessary for safety and safe delivery shall be provided.

APPENDIX A: Cavity TEM$_{00}$ Diffractive loss

1. Discussion of Table 2.

Row 3 in table 2 is intended to give a simple geometrical feel for the COC diameters with respect to the Gaussian cavity beam intensity. The diameters presented are those where an exact TEM$_{00}$ Gaussian cavity beam at the optic's location has fallen to 10^{-6} of its center intensity. If w_{xx} is the Gaussian beam radius at the optic's location then the diameters are equal to $5.257 w_{xx}$. For instance, in the recycling cavity, where the Gaussian radius is $w_{RM} = 4.65$ cm, the 1ppm diameter= (4.65)(5.257)= 19.2 cm (for normal incidence).

The BS presents a special situation: loss is dominated by the outer edge clipping of the *in-line* split off beam (since it is not centered on the exit (AR) optic face. This fact suggests a compromise where the beam is decentered on the BS entrance (ER) surface. Figure A.1 shows this dependence: a ~1 cm decentering is optimal. Of course, such decentering *increases* the dark port beam loss (to ~400 ppm for 1 cm decenter).
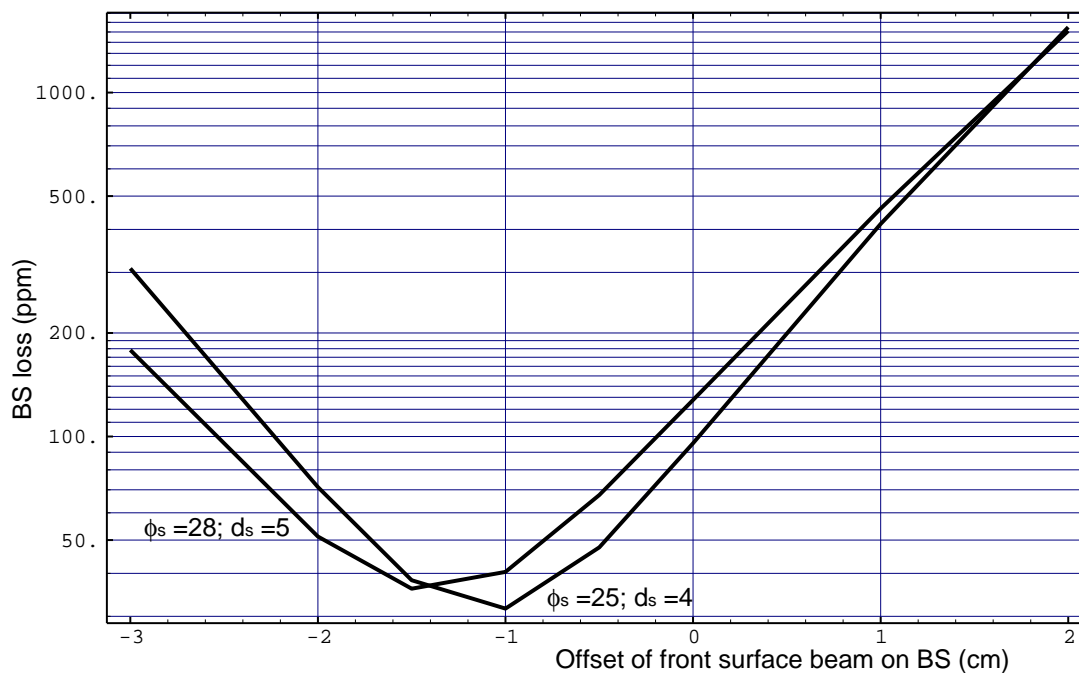
Figure A.1 Total geometrical clipping loss of beams impinging on BS. Illustrates that net loss

can be minimized with offset. Both the case of Table 2 and the alternative case of Appendix

L are shown. For these calculations ϕ_e (effective optical diameter) = 24 and 27 cm were used.

Since relatively large losses are encountered at the BS, it is important to understand the disposition of this lost light. Figure A.2 shows what portion of the in-line beam power ultimately impinges on the substrate cylindrical walls (and presumably is then lost to an uncontrollably large solid angle)
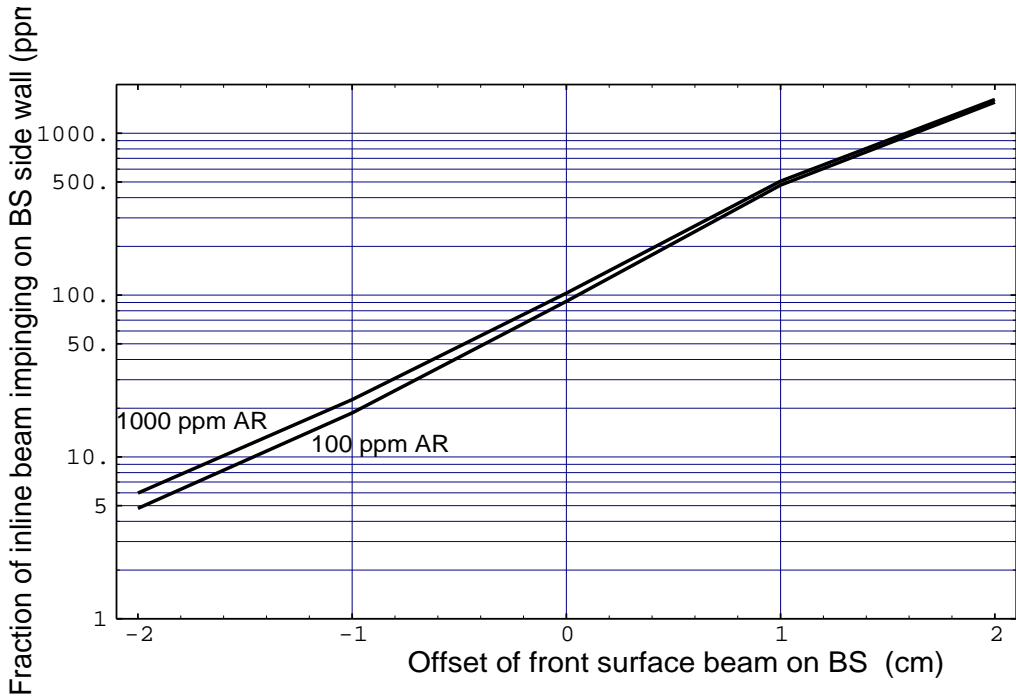
.

Figure A.2 Plotted is walk off (only energy impinging on substrate cylindrical sides) loss

of in-line beam through BS. Case of Table 2. For these calculations ϕ_e = 24 and 27 cm were used.

As a follow up to these geometrical studies of loss, FFT code modeling was performed to study the effect of beam splitter clipping for various BS diameters. Figure A3 summarizes those studies. Curve 1. is for the case of ϕ_s =28

Offset of Front Surface Beam on Beam Splitter (cm)
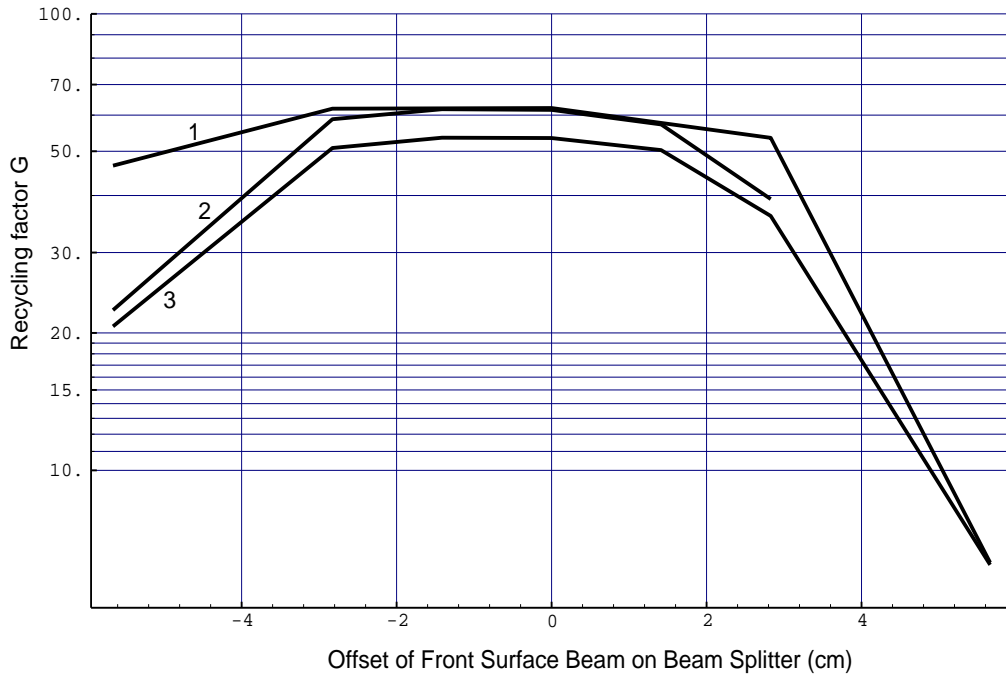
cm, d_s= 5 cm, with Calflat mirror surface maps and 50 ppm base loss per mirror surface. Curve 2 and 3 are for ϕ_s =25 cm, d_s= 4 cm. Curve 2 employs the same mirrors as Curve 1. Curve 3 uses the same set of mir-

ror maps but degraded by a factor 2/3. We conclude from this that even ϕ_s =28 cm, d_s= 5 cm mirrors allow for an adequate centering tolerance margin, as evidenced by the ~ 4 cm flat top to the corresponding G_R curves.

2. Disk mirror diffractive loss.

For the 4000 m cavity with g= 0.3 Spero (LIGO note #110- 2/28/92) has calculated the diffractive loss from mirrors which are ideal up to a sharp diameter edge D(α) where α is the fractional loss. For cases of interest in this document it turns out that this exact calculation gives diameters (say for $\alpha= 10^{-6}$) < 1% greater than the naive geometrical one of 1. above. Thus we can take the naive truncated Gaussian model as an accurate estimator of beam tail loss. The relevance of a ~1ppm loss criteria for mirror diameters is a more important consideration. At 1064 nm micro-roughness scattering plus surface absorption loss at the critical arm cavity mirrors may likely be no more than a few tens of ppm (see 3.2.1.5). Thus it is reasonable to insist, at least, that mirror diameter diffraction loss be < this order. Now for $\alpha= 10$ ppm D= 26.5 cm for the ETM, so allowing for 0.9cm centering and 0.6cm bevel, ~ 28 cm diameter mirrors will still be required.

3. **FFT study of mirror diameter effect.**

Preliminary studies have been performed with the FFT code model at 1064 nm with various ETM diameters (where the mirror is modeled with R= 1.00 to the edge). With respect to carrier light loss (essentially in the arm cavities) these runs support the loss estimates and scaling of 2. above. In several comparisons between 25 cm and 30 cm mirror diameters, G_R was 20-30% reduced for the smaller ETM diameter. This fractional reduction was most pronounced in the case of 50 ppm loss per surface mirror quality (as compared to 100 ppm). This clearly indicated that mirrors significantly larger than 25 cm diameter are required for LIGO shot noise performance to be limited by mirror surface quality alone.

FFT runs in the same series show virtually no G_R improvement for diameters larger than 30 cm (34 cm specifically). In fact we see that ~30 cm diameter represents a weak optimum in the sense that beyond this diameter contrast defect grows due to the increased fraction of imperfection generated higher transverse mode power which remains in the arm cavities and hence escapes back to the dark port.

APPENDIX B: Scaling of thermal noise tail

1. 1064 nm numerical calculation

The TM thermal noise contribution to IFO sensitivity well below ν_0 (internal) is determined by the tails of the thermal noise driven internal resonances. For 25 cm diameter, 10 cm thick TMs and 1064 nm the appropriately weighted sum over modes was supplied by K. Blackburn (private communication, Feb. 1996. The data of table 3 and figure 6 are based on this calculation/extrapolation.

2. Similar calculations

Exact calculations of TM thermal noise for 1064 nm and slightly different mirror dimensions have been published by VIRGO investigators (F. Bondu, J-Y Vinet, Phys Lett **A 198**, 74). These calcu-

lations show that, for cases very close to the geometry of table 2, the contribution of the ITM dominates by 3-4 (in spectral power density) over that of the ETM, and has approximately the same value as the case used in C.1.1 of LIGO-T95011-01.

APPENDIX C: Internal mode frequencies vs dimensions
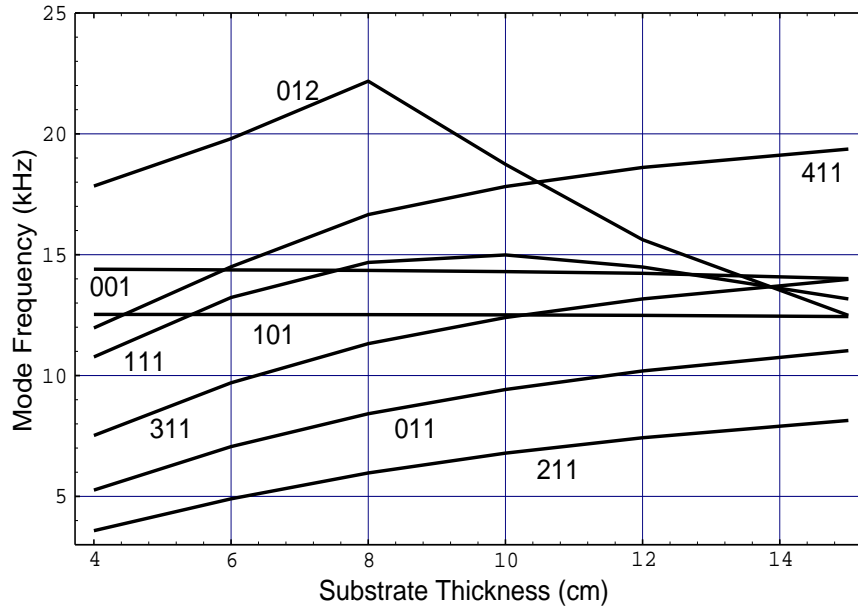
1. ETM mode frequencies vs thickness.

Figure C1: Plot of the lowest mode resonant frequencies as a function of thickness for 25 cm diameter fused silica substrates. (K. Blackburn numerical code, 2/96)
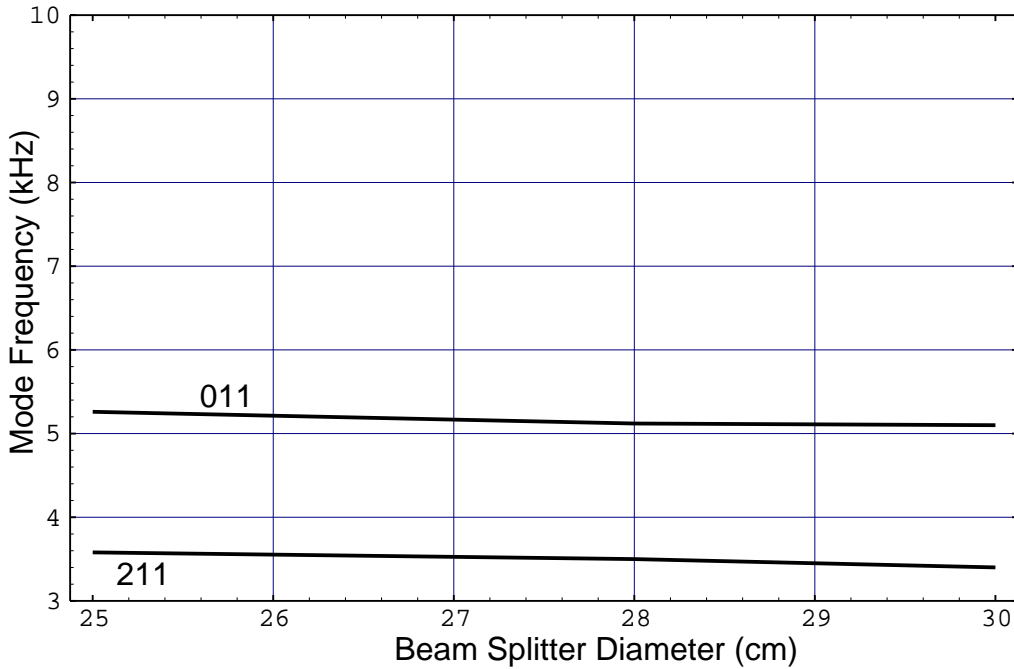
2. BS mode frequencies vs diameter.

Figure C2: Principle lowest two mode frequencies for the BS as a function of diameter where thickness is constrained such that the impinging beam 100 ppm intensity contour (as per A.1) is contained within a circle 1.50cm in diameter less that the substrate diameter. One sees that this constraint does not allow higher frequency lowest resonances (K. Blackburn, 2/96).

APPENDIX D: Nominal coating values:

1. ERITM reflectivity

The arm cavity storage times (nominally $8.8 \cdot 10^{-4}$ sec.) should be matched to provide laser frequency noise suppression. This has been discussed in LIGO-T950030-03-D (appendix.2) where it is shown that a fractional storage time difference of ~0.01 is adequate to suppress residual frequency noise in the servo locked IFO. For small transmission values, the corresponding limit on ITM transmission match is equal to this.

If the arms are not matched optically they will have different mean TEM_{00} cavity power. Amplitude fluctuations in the IFO laser beam will cause different absolute power fluctuations in the arm cavities, in ratio equal to the ratio of the mean powers. Therefore the radiation pressure fluctuation on the TMs due to any laser amplitude fluctuation will not be exactly balanced as a common mode "signal". The resultant unbalanced IFO displacement noise will be proportional to the ERITM fractional reflectivity difference and is (for the substrates of table 2; suspensions as described in LIGO-T9500xx-01-D; 6 Watts laser power into the IFO with an amplitude noise spectrum as in LIGO-T950030-03-D (appendix.4); and the transmission tolerance of 3.2.1.3.1,

$$z_{rms}(100 \text{ Hz}) \leq 1.4 \text{ x } 10^{-22} \text{ meter/Hz}^{1/2}$$

Unbalanced arm cavities can also contribute to contrast defect. For instance a cavity with loss L and field reflectivity r, sends back a field $\sim E_0(1 - L/(1-r))$ to the beam splitter. For a lossless sec-

ond arm this gives CD= $0.5(L/(1-r))^2 < 10^{-4}$ for anticipated L (section 3.2.1.5). For the case of balanced losses and a fractional difference in r between the arms CD will be even smaller.

2. ERRM reflectivity

The ERRM coating reflectivity is chosen to critically couple the IOO laser beam carrier component into the full recycled IFO. The recycling gain function $G_c(r_{RM})$ is highly asymmetric about the criticality maximum. Therefore the tolerance required on $r_{RM,max}$ will be asymmetric. Using the criterion that any deviation from $r_{RM,max}$ not reduce G_R by more than 2% one finds that for a typically modeled LIGO situation ($r^2_{RM,max}$=.97, $G_R \sim 34$) that the reflectivity tolerance is +.005/-.01, which is quite loose.

A more subtle, but perhaps quite important, influence on this reflectivity choice is allowance for degradation of IFO performance with time. If $r_{RM,max}$ is chosen for an initial low loss configuration of the IFO then if overall IFO losses increase over time the laser will become undercoupled into the IFO and G_R can fall off rapidly. Two cases for realistic LIGO parameters were modeled, one with 50 ppm and the other with 100 ppm mirror losses. If $r_{RM,max}$ is chosen for the 50 ppm case then the reduction in G_R as the losses increase to 100 ppm will be ~10% more than would be if $r_{RM,max}$ were initially chosen for 100 ppm loss. The actual reflectivity shift this represents is ~.006, within the tolerance presented in the last paragraph. This argues for an even greater tolerance asymmetry.

3. ERBS splitting

Assume a perfect BS (here, for the sake of discussing the split requirement) with $t^2 + r^2 = 1$ which is preserved with the parameterization $t = 2^{1/2}(1 + 2\varepsilon)^{1/2}$ and $r = 2^{1/2}(1 - 2\varepsilon)^{1/2}$. Then the cancelation at the dark port does not depend on ε. The visibility does however, the GW signal being $\propto (1 - 4\varepsilon^2)^{1/2}$. This is only a very loose constraint.

More relevant is the desire to keep the absolute power levels of both arms the same. Since thermal distortions (film and bulk) are $\propto P$ and the power scattering (to HTMs) of such distortions is as their square, net thermal induced scattering is $\propto P^3$.

APPENDIX E: Mode Spectrum Tolerance

If g_i for the two TMs vary (due to variation of R_i from the nominal values of Table 2, the phase spectrum of arm cavity modes is modified as in Figure E.1. The smooth curve in this figure is the power enhancement factor for an arm cavity with 400 ppm total loss and R = 0.97 input mirror. Superimposed on this are points (small dots) at the position of the Guoy phase of the first ten higher transverse modes (with non-degenerate phase values) for the exact design: g_1g_2 =1/3. For modes with power factors < 1, their field is suppressed with respect to free space. The larger dots are the spectrum of these same ten modes with $\Delta g_1/g_1$ = -.02. The only large change (by ~2x) in
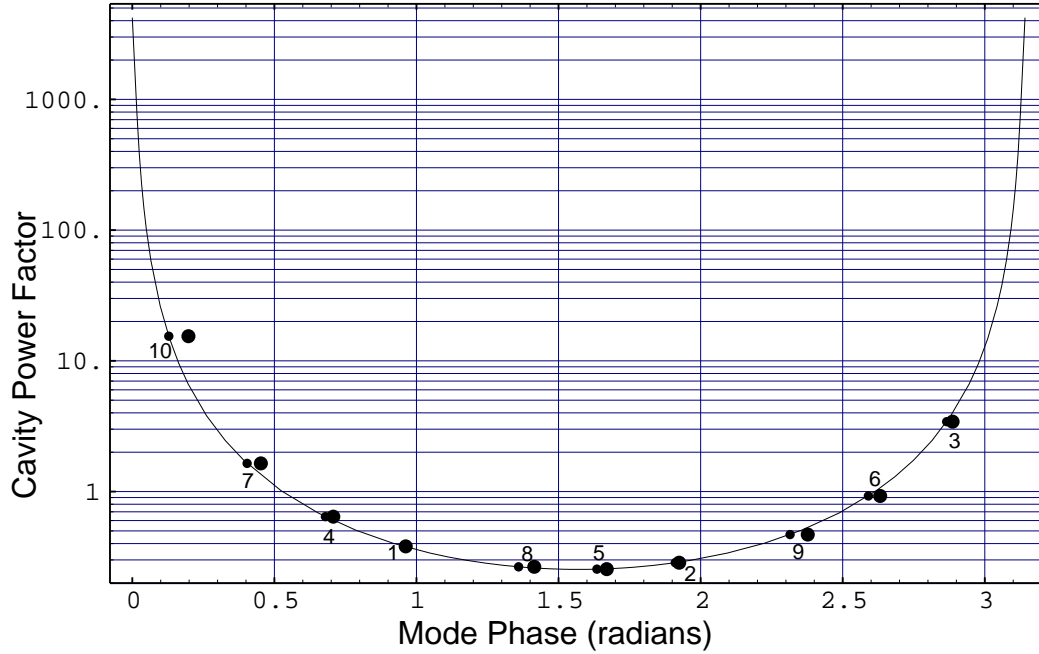
power factor occurs for mode 10.

Figure E.1 Transverse mode spectrum (dots) for Table 2 arm cavities. Modes are labeled as

multiples of the basic cavity round trip Guoy phase.

APPENDIX F: Effective curvature matching

1. Parabolic mirrors- Flat/Curved cavity

For mirrors with only parabolic shape (no other figure errors) the definition of R_{eff} is unambiguous: it is the local surface curvature at *any* point on the surface. The IOO laser beam can, in general, be tuned to mode match into one [arm] cavity. Then we calculate the contribution to CD resulting from the mismatch into the other arm. The simplest case is for identical arms except for a ΔR in the ETMs (surface 1). For the ETM mirrors the value in table 4 is $\Delta R/R$. Since this is small we proceed perturbatively (see the cavity mode matching discussion in D.Z. Anderson, Appl. Opt., **23**, 2944 (1984). The mismatched portion of the input TEM_{00} wave is represented as the next highest order axisymmetric Laguerre-Gauss mode $LG_{1,0}$ (the only one with parabolic matrix element coupling to $LG_{0,0}$). The power in $LG_{1,0}$ returning to the dark port gives:

$$CD_c = 2 \left(\frac{(1+\chi)}{4\chi} \right)^2 \left(\frac{\Delta R}{R} \right)^2$$

Where $\chi = \left(\frac{\pi w_0^2}{\lambda L} \right)^2 = 1/2$ for g = 1/3. For $\Delta R/R = .015$ this gives $CD_c = 2.5 \ 10^{-4}$. For $1/R_{eff} > 0$ on the

ITM mirrors the much smaller contribution is:

$$\mathrm{CD_c} = \frac{1}{4}\left(\frac{6000\mathrm{m}}{R_{eff}}\right)^2\left(\frac{1-\chi}{1+\chi^2}\right)^2$$

2. Parabolic mirrors- Curved/Curved cavity

This general situation is more complicated, with two solutions possible ($g_{1,2} <$ or > 0) given the Guoy phase and L. It is described in figure F.1. The fractional change in $LG_{1,0}$ mismatch power due to an error $\Delta R_{ETM,eff}$ is plotted (I in Fig. F.1) normalized to $(\Delta R_{eff}/R_{ETM})^2$. For instance for
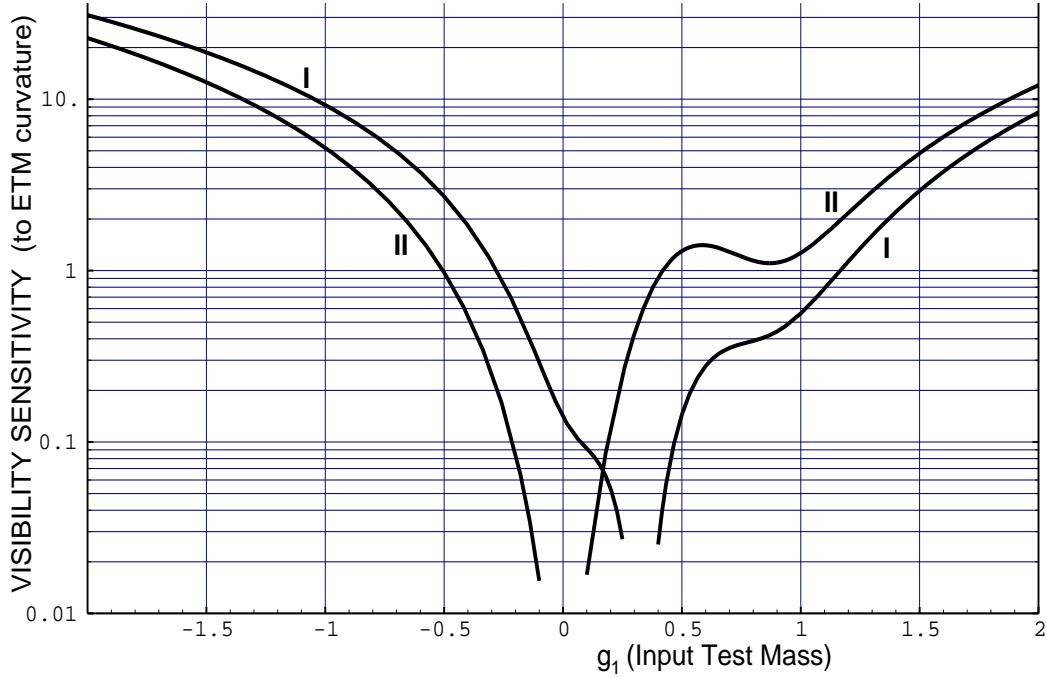

Figure F.1 Differential power matching ("Visibility") is plotted with respect to g_{ITM}. The reference

point is constrained to $g_1 g_2 = 1/3$. Sensitivity to $\Delta R_{ITM,eff}$ is had from the values at $g_1 = g_{ETM}$.

the case of the last paragraph, $g_1 = 1$, the plot shows $CD_c/2$. A symmetric Curved/Curved cavity would correspond to $g_1 = \pm 3^{-1/2} = 0.577$ and we see that the choice + has much less mismatch sensitivity to curvature error (as do slight variations from symmetry, as in table 2). Curve || in the figure is the same but with normalization to $(\Delta h_{ETM})^2$ with h_{ETM} the mirror sagitta (perhaps a better criterion for practical optic fabrication).

APPENDIX G: FFT model of central surface errors

Table 11 presents results from a series of FFT runs at 1064 nm for a band of plausible LIGO cases. Mirror quality is varied with respect to two parameters; L_m = per mirror "base loss" (same for all mirrors-see 3.2.1.5.3) and mirror central figure error (3.2.1.4.2). The label "λ_{900}" means that the run used [all] mirror surfaces [and substrates] of quality called "$\lambda/900$" in the original FFT program designation. λ_{600} and λ_{400} pertain to the same convention except that their substrates are not altered (from the "$\lambda/900$" runs). All runs used perfect beam splitters, assumed a flat-

curved arm cavity geometry, and had mirror apertures of 30 cm diameter (so that optical aperture clipping is presumably negligible).

Table 11: Summary of 1064 nm FFT results

FFT result	$L_m = 50$ ppm				$L_m = 100$ ppm			
	λ_{400}	λ_{600}	λ_{900}	perfect	λ_{400}	λ_{600}	λ_{900}	perfect
$1 - C \times 10^{-3}$	1.4	.61	.27	0.	1.5		.28	0.
$h(0) \times 10^{-23}$	1.07	.83	.77		1.33		1.02	
$h(100) \times 10^{-23}$	1.6	1.24	1.16		2.1		1.5	
G_R	37.1	51.5	62.4	75.0	24		34.4	37.9
$P_{missing}/P_0$	.49	.30	.17	~ 0	.53		.09	~ 0

The notion of "missing power", $P_{missing}$ is invoked here. Normalized to P_0, the laser power input to the RM, it is the fraction of P_0 which is not explicitly accounted for in the FFT code by 1) $\Sigma L_m * P_m$ (where P_m is the power impinging on mirror m); 2) Power leaking back out the RM (negligible in all optimized runs); 3) Power "lost" to transmission through the ETMs ;and 4) power,as contrast defect, leaking out the dark port. Only carrier power is considered in this fraction.

APPENDIX H: Micro-roughness and scatter loss

In principle 3.2.1.5.3 and 3.2.1.4.4 are the same requirements. For "smooth surfaces", defined as surface roughness amplitudes $<< \lambda_{laser}$, and for surface scales $\lambda_s <$ few mm where isotropy and short correlation lengths of imperfections presumably hold, scattered power and micro-roughness are related by:

$$\frac{\Delta P_{scattered}}{P_{incidend}} = \left(4\pi\frac{\sigma}{\lambda_{laser}}\right)^2$$

For a a surface micro-roughness (rms), σ, $= 0.4$nm this relation gives 22 ppm scattered loss (1064nm). However it will be difficult to establish that any specific measurement of σ is appropriate for a certain intended regime of ΔP_{scatt}. For instance sample mirrors (REO ring-down test data c 7/95) can have net scatter + absorption losses ≤ 2 ppm at 514 nm (Boccara, et. al.,J. Phys IV, C7-631, 1994 also report absorption in similar coatings at 1064 nm to be ≤ 1 ppm). The above relation then implies $\sigma_{eff} = 0.057$ nm corresponding to the best superpolish. Partial explanation of this lies in the fact that the method for determining this ≤ 2 ppm figure involves cavities with w $<$ λ_s scale of interest

APPENDIX I: Balanced/unbalanced lensing

1. **ITM case.** An extensive study of this problem has been published by VIRGO collaborators (Hello and Vinet, Phys. Lett. **A**   **).** A full understanding of the implications of these results is TBD. The lowest order [matching] effect of lensing has been formulated by W. Winkler, et. al, (Phys. Rev. **A44**, 7022). Here I simply compare this lowest order estimate of the thermally induced OPD_w (beam center to beam w radius) to the P.V. ITM OPD levels already incorporated into the FFT models runs. Winkler, et al gives $OPD_w = 1.3P\ d_s L_{th}\beta/4\pi\kappa$ where P is the beam power through the optic, β is the index thermal coefficient, L_{th} is the specific absorption,and κ is the thermal conductivity. For L_{th}= 15 ppm/cm (~Corning 7940 FS) and P=160 Watts, $OPD_w = \lambda_{633}/37$ which is about three times smaller than the P.V. OPD used for ITM distortion in the FFT distortion of Table 12 column 3 (also the basis of distortion requirements for table 4 and sections 3.2.1.5 and3.2.1.3).

2. **BS case**. Lensing plays an obviously asymmetrical role for the two arms (assuming that the BS splitting surface is spaced from the dark port by the optic's bulk): one arm sees no lens while the other does, in double pass. The recombined beam then also is lensed (assumed to be a negligible effect). Pending an understanding/agreement with the VIRGO work it may be advantageous to design a symmetrical BS^{TBD}. It is not obviously superior , from the point of view of thermal lensing, to have the splitting coating face the dark port.

3. **Bulk "microlensing".** Sections 3.2.1.4 and 5 only consider long λ_s bulk imperfections. The case of $\lambda_s <$ few mm is considered in the thesis of P. Hello (appendix II) where it is found that the rms phase front distortion caused by such inhomogeneity roughness has as stringent a limit requirement as that for mirror surface rms imperfections.

APPENDIX J: Recycling cavity element error effects.

APPENDIX K: Diffraction Loss mechanisms.

Table 12: Higher transverse mode loss relative to TEM$_{00}$

Symmetric Laguerre-Gauss mode	$LG_{0,0}$	$LG_{1,0}$	LG_{20}	$LG_{3,0}$	$LG_{4,0}$	$LG_{5,0}$
Geometrical Loss	10^{-6}	$1.5\ 10^{-4}$	$5\ 10^{-3}$	$6\ 10^{-2}$	0.27	0.46
Cavity Res. factor	1	0.29	0.65	0.93	0.27	16.1

Table 13: ETM diameter effect on diffraction losses

ϕ_e (cm)	100ppm; λ_{633}/900 mirrors				50ppm; λ_{633}/600 mirrors			
	CD_c x10^{+4}	G_R	$P_{00,arm}$/P_{IO}	L_{diff}	CD_c x10^{+4}	G_R	$P_{00,arm}$/P_{IO}	L_{diff}
25	2.9	28	1812	16	14.6	23	1466	59
30	2.8	34.5	2230	8	13.7	30	1944	46
34	3.7	33.9	2205	9				

APPENDIX L: An Alternative COC parameterization

If we do not insist on a requirement that all COC ϕ_s be the same then it is of interest to consider a case which may be regarded as the minimal relaxation of that constraint. This is done by identifying the BS as the single element which should be a "special" ϕ_s since, for the parameterization of table 2, it is the most geometrically lossy element. A specific example is presented in table 13. Features (bad and good) of this configuration are:

- Being symmetric, the arm cavities require one less polished substrate type. However, since the ITM and ETM are otherwise different (FS type, coating) this feature does not reduce total type count.
- Since the 2000m IFO configuration of section 3.2.1.7 is already symmetric there are virtually no changes in its performance for the COC sizes of table 13.
- The maximum laser beam intensity impinging on a COC is 21% less than for table 2 (larger ITM beam radius).
- The lowest few substrate internal mode resonance frequencies are nearly the same as for the table 2 configuration.
- The COC weights are very significantly reduced. TMs are 36% lighter than those in table 2. This could be a major benefit in handling, cleaning, mounting, fabrication, etc.
- Significantly less face edge margin is available (e.g. for OSEMs) on the ITM. Mounting this element would require some special consideration.
- The specific BS ϕ_s of table 13 has a slightly higher(30%) geometrical clipping loss than that of table 2. The two cases are compared in figure A.1. This figure may also be used to accurately estimate the geometrical loss for other BS ϕ_s by assuming offset to be ~equivalent to change in substrate radius. The conclusion is that $\phi_s \geq 30$ cm would be required to make this loss significantly less (< 20 ppm).

Table 14: Alternate, Symmetric Arm cavity configuration (4000m IFO)

Physical Quantity	Test Mass ITM	ETM	Beam splitter	Recycling mirror
Diameter of substrate,ϕ_s (cm)	22.5	22.5	28	22.5
Substrate Thickness, d_s (cm)	8	8	5	8
1 ppm intensity contour diameter (cm)[a]	21.4	21.4	33[b]	21.5
Lowest internal mode frequency (kHz)	6.83	6.83	3.50	6.83
Weight of Suspended Component (kg)	6.9	6.9	6.2	6.9
Wedge angle (Surf. 2)[TBD]	$\leq 3^o$	$\leq 3^o$	$< 1^o$	$\leq 3^o$
Nominal surface 1 radius of curvature (m) and g_i factor	9464 g_1=.577	9464 g_2=.577	∞	6438 g=.9975

a. See Appendix A for exact definition.

b. For these 45° angle of incidence optics, this is the smallest diameter circle centered on the optic face which is everywhere outside of the 1 ppm intensity field.